LEARNING GRAPH REPRESENTATIONS VIA GRAPH ENTROPY MAXIMIZATION

Anonymous authors
Paper under double-blind review

ABSTRACT

Graph representation learning aims to represent graphs as vectors that can be utilized in downstream tasks such as graph classification. In this work, we focus on learning diverse representations that can capture the graph information as much as possible. We propose to quantify graph information using graph entropy, where we define a probability distribution of a graph based on its node and global representations. However, computing graph entropy is NP-hard due to the complex vertex packing polytope involved in its definition. We therefore provide an approximation of graph entropy based on the Shannon entropy and the chromatic entropy. By maximizing the approximation of graph entropy through graph neural networks, we obtain informative node and graph representations. Experimental results demonstrate the effectiveness of our method in comparison to baselines in unsupervised learning and semi-supervised learning tasks.

1 INTRODUCTION

Graphs, such as chemical compounds (Debnath et al., 1991; Kriege & Mutzel, 2012), protein structures (Borgwardt et al., 2005), and social networks (Yanardag & Vishwanathan, 2015), represent relationships between various entities. Graph representation learning aims to convert graph-structured data into effective vector representations for various downstream tasks like graph classification. This task is nontrivial because graph data are non-Euclidean data. There have been many works of graph representation learning using the GNNs (Kipf & Welling, 2016a; Hamilton et al., 2017a; Xu et al., 2018; Veličković et al., 2017; Kipf et al., 2018; Xie & Grossman, 2018; Gilmer et al., 2017). Unsupervised graph-level representation learning is a fundamental and challenging task in this field. For example, InfoGraph (Sun et al., 2019) achieves graph-level representations by maximizing mutual information between graph-level representations and node-level representations. Graph contrastive learning (GraphCL) (You et al., 2020) and adversarial graph contrastive learning (AD-GCL) (Suresh et al., 2021) obtain graph-level representations by training GNNs to maximize the correspondence between representations of the same graph in different augmented forms. JOint Augmentation Optimization (JOAO) (You et al., 2021) is a framework that automatically and adaptively selects data augmentations for GraphCL on specific graph data using a unified bi-level min-max optimization approach. Automated Graph Contrastive Learning (AutoGCL) (Yin et al., 2022) utilizes learnable graph view generators and an auto-augmentation strategy to generate contrastive samples while preserving the most representative structures of the original graph. Graph Adversarial Contrastive Learning (GraphACL) Luo et al. (2023a) introduces a novel approach to self-supervised whole-graph representation learning by learning negative samples. InfoGCL Xu et al. (2021) delves into the transformation and transfer of graph information within the contrastive learning process, introducing an information-aware framework for graph contrastive learning. Spectral Feature Augmentation (SFA) Zhang et al. (2023) offers an efficient spectral feature augmentation method for Graph Contrastive Learning (GCL). Graph Contrastive Saliency (GCS) Wei et al. (2023) focuses on identifying semantically discriminative substructures within graphs through contrastive learning. Neighbor Contrastive Learning Augmentation (NCLA) Shen et al. (2023) enhances graph augmentation through neighbor contrastive learning. Simple Neural Networks with Structural and Semantic Contrastive Learning (S^3-CL) Ding et al. (2023) learns expressive node representations in a self-supervised manner. Imbalanced Node Classification (ImGCL) Zeng et al. (2023) automatically balances learned representations from GCL without labels.GRADATE Duan et al. (2023) presents a comprehensive framework for Graph Anomaly Detection, incorporating subgraph-subgraph contrast and augmented views into multi-scale contrastive learning networks. These graph-level representation learning methods are all based on the InfoMax principle (Linsker, 1988). It is important to note that there are several other graph representation learning methods, such as VGAE (Kipf & Welling, 2016b; Hamilton et al., 2017b; Cui et al., 2020), graph embedding methods (Wu et al., 2020; Yu et al., 2021; Bai et al., 2019; Verma & Zhang, 2019), self-supervised learning (Sun et al., 2023; Liu et al., 2022b; Hou et al., 2022; Lee et al., 2022; Xie et al., 2022; Wu et al., 2021; Rong et al., 2020; Zhang et al., 2021b;a; Xiao et al., 2022), and contrastive learning (Le-Khac et al., 2020; Qiu et al., 2020; Ding et al., 2022; Xia et al., 2022; Fang et al., 2022; Trivedi et al., 2022; Han et al., 2022; Mo et al., 2022; Yin et al., 2022; Xu et al., 2021; Zhao et al., 2021; Zeng & Xie, 2021; Li et al., 2022a;b; Wei et al., 2022). Due to the page length limitation, we will not detail these methods.

In the past decades, a variety of notions of entropy have been proposed for measuring the information and complexity of graphs from different aspects (Dehmer & Mowshowitz, 2011; Dehmer, 2008). For example, the structural entropy (Mowshowitz & Dehmer, 2012) is defined on the Shannon entropy and the structural components of each node (e.g. the degree of a node). The structural entropy is widely used in GNN-based graph learning methods for measuring the topological structural information of graphs (Luo et al., 2021; Yang et al., 2023; Wang et al., 2023; Wu et al., 2022; Zou et al., 2023; Fang et al., 2021). The edge entropy is defined on the connected structure of edges and is also used to evaluate the structural information of graphs (Jiang et al., 2020; Wang et al., 2021; Grebenkina et al., 2018; Aziz et al., 2020; Luo et al., 2023b). The von Neumann entropy of a graph is defined on the graph Laplacian and is used to measure the spectral complexity of graphs (Liu et al., 2021; 2022a; Passerini & Severini, 2008; Minello et al., 2019; Ye et al., 2014; Dong et al., 2019). The Rényi entropy is a generalized information measure including various notions of entropy and is used for graph clustering tasks (Pál et al., 2010; Oggier & Datta, 2021). M-ILBO Ma et al. (2023) involves the estimation of graph dataset entropy by maximizing the Information Lower Bound (ILBO) using subsets of data samples. However, it's important to clarify that while these works use the term "graph entropy", they are not referring to the authentic Graph entropy as defined by János Körner (Körner, 1973). Graph entropy is, in fact, a fundamental concept deeply rooted in the disciplines of combinatorics and information theory, with a rich history. In 1948, Claude E. Shannon laid the foundations of information theory and introduced the concept of channel capacity (Shannon, 1948). Subsequently, in 1973, János Körner introduced the concept of graph entropy, which serves as a measure of the information that can be effectively communicated over a noisy channel (Körner, 1973). While graph entropy finds its origins in information theory, it also finds utility in quantifying the information within a set, especially when some pairs of elements share common information (Bouchon et al., 1988). In 1979, László Lovász introduced orthonormal representations with the aim of analyzing a graph's Shannon capacity (Lovász, 1979). These representations comprise sets of vertex representation vectors, allowing for the possibility that adjacent vertices may share common information. This property aligns with the combinatorics definition of graph entropy. Nevertheless, the computation of graph entropy becomes a computationally challenging task due to the complex vertex packing polytope involved in its definition.

While graph entropy has found success in the realms of combinatorics and information theory, it remains relatively unexplored within the field of graph learning. In this study, we introduce a novel approach called Graph Entropy Maximization (GeMax) for graph representation learning, marking the first instance of its application in this context. Our approach begins with two key insights: firstly, the necessity of employing orthonormal representations for nodes, which enables direct measurement of the information contained in graph representations using graph entropy. Secondly, we establish a probability distribution for a graph by incorporating its nodes' representations and a global graph representation learned through two separate graph neural networks. Recognizing the computational challenges associated with graph entropy, we propose an approximation method that leverages Shannon entropy and chromatic entropy. This approximation leads to a max-min optimization problem, which we address through alternating minimization techniques. Through extensive experimentation, we validate the competitiveness of our proposed methods against various baselines in both unsupervised graph-level and node-level learning tasks. In summary, our contributions in this work can be categorized into three main areas.

- We introduce a novel method, Graph Entropy Maximization (GeMax), for graph representation learning, marking the inaugural exploration of Körner's graph entropy within the graph learning community.

- Our framework for employing Körner's graph entropy consists of two key components: firstly, the adoption of orthonormal representations for nodes, facilitating direct quantification of information within graph representations through graph entropy. Secondly, the establishment of a probability distribution for a given graph.
- Additionally, we present an approximation technique to compute graph entropy, leveraging both Shannon entropy and chromatic entropy.

2 Preliminaries

In this section, we introduce the definitions of orthonormal representations, graph entropy and chromatic entropy. The main notations used in this paper are shown in Table 5 of Appendix A.1.

2.1 orthonormal representations

Given a graph $G = (V, E)$, if two vertices share some information and may be confused in communication, they are adjacent with an edge. In contrast, if there is no common information between two vertices, they should be non-adjacent. Based on this intuition, László Lovász introduced the orthonormal representations of a graph (Lovász, 1979). If two vertices are non-adjacent, Lovász argued that their representation vectors should be orthogonal to each other, indicating that there is no common information between them.

Definition 2.1 (Set of orthonormal representations (Lovász, 1979))**.** Given a graph $G = (V, E)$, we use a unit vector $\boldsymbol{z}_i \in \mathbb{R}^d$ to denote the d-dimensional representation of vertex i. Then the set of orthonormal representations of G is defined as

$$\mathbb{T}(G) := \{\boldsymbol{Z} \in \mathbb{R}^{d\times n} : \|\boldsymbol{z}_i\|_2 = 1, i = 1, 2, \ldots, n;\ \boldsymbol{z}_i^\top \boldsymbol{z}_j = 0,\ \forall (i,j) \notin E\}. \tag{1}$$

2.2 Graph Entropy

Graph entropy is a fundamental property of a probabilistic graph, first introduced by Körner (1973). Though there exist several equivalent definitions of graph entropy, we focus on its combinatorial definition which is based on the vertex packing polytope VP(G). In graph theory, the independent set is a set of vertices of $\mathcal{G}$ where no two vertices are adjacent. Let $\boldsymbol{B} = [\boldsymbol{b}_1, ..., \boldsymbol{b}_{N_b}] \in \{0,1\}^{|V|\times N_b}$ be the indicator matrix of independent sets of G, where N_b is number of independent sets of G and the i-th column $\boldsymbol{b}_i$ is the indicator vector of the i-th independent set. For example, if G is a pentagon in Figure 1, we have $N_b = 10$ and $\boldsymbol{b}_6 = [1, 0, 1, 0, 0]^\top$ indicates the vertex subset $\{v_1, v_3\}$ is the 6-th independent set of G. The vertex packing polytope VP(G) is defined as follows.

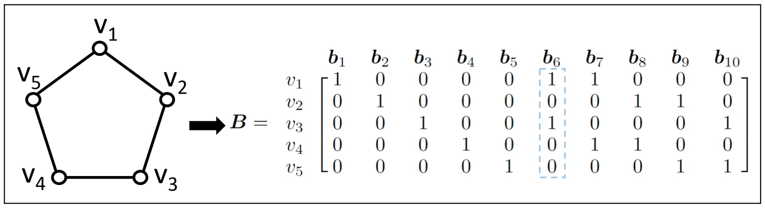

$$\boldsymbol{B} = \begin{array}{c|cccccccccc} & \boldsymbol{b}_1 & \boldsymbol{b}_2 & \boldsymbol{b}_3 & \boldsymbol{b}_4 & \boldsymbol{b}_5 & \boldsymbol{b}_6 & \boldsymbol{b}_7 & \boldsymbol{b}_8 & \boldsymbol{b}_9 & \boldsymbol{b}_{10} \\ \hline v_1 & 1 & 0 & 0 & 0 & 0 & 1 & 1 & 0 & 0 & 0 \\ v_2 & 0 & 1 & 0 & 0 & 0 & 0 & 0 & 1 & 1 & 0 \\ v_3 & 0 & 0 & 1 & 0 & 0 & 1 & 0 & 0 & 0 & 1 \\ v_4 & 0 & 0 & 0 & 1 & 0 & 0 & 1 & 1 & 0 & 0 \\ v_5 & 0 & 0 & 0 & 0 & 1 & 0 & 0 & 0 & 1 & 1 \end{array}$$

Figure 1: The indicator matrix $\boldsymbol{B}$ of independent sets of a pentagon

Definition 2.2 (Vertex packing polytope)**.** Given a graph G with vertex set V, the vertex packing polytope VP(G) of G is the convex hull of the indicator vectors of its independent sets. More precisely, let $\boldsymbol{B} \in \{0,1\}^{|V|\times N_b}$ be the indicator matrix of independent sets of G and $\boldsymbol{\lambda} \in \mathbb{R}_+^{N_b}$ be a vector, then VP(G) is defined as follows

$$\text{VP}(G) := \left\{ \boldsymbol{a} \in \mathbb{R}^{|V|} : \boldsymbol{a} = \boldsymbol{B}\boldsymbol{\lambda},\ \text{with } \boldsymbol{\lambda} \geq 0, \sum_{i=1}^{N_b} \lambda_i = 1 \right\}. \tag{2}$$

Let (G, P) be a probabilistic graph with respect to probability distribution P on its vertex set V, i.e., $P = \{P_1, P_2, ..., P_n\}$ and P_i is the probability density of the vertex i. The graph entropy is usually denoted as $H_k(G, P)$, named after János Körner. Based on VP(G), we have

Definition 2.3 (Graph entropy Körner (1973)). Given a probabilistic graph (G, P) with $|V| = n$, the entropy of G with respect to P is defined as

$$H_k(G, P) := \min_{\boldsymbol{a} \in \text{VP}(G)} \sum_{i=1}^{n} -P_i \log(a_i), \tag{3}$$

where $\boldsymbol{a}$ is a vector in the vertex packing polytope VP(G) and a_i is the i-th element of vector $\boldsymbol{a}$.

In information theory, the graph entropy is a measure of the maximal information rate of communicating over a noisy channel. This notion has been extended to combinatorics as follows.

Corollary 2.4 ((Bouchon et al., 1988)). *In combinatorics, graph entropy can be used to measure the amount of information contained in a set where some pairs of elements contain common information.*

It is known that a graph is a set and its vertices are the elements, where adjacent vertices contain common information. Thus, according to Corollary 2.4, **graph entropy can be used to measure the amount of information contained in the orthonormal representations of a graph**.

2.3 Chromatic Entropy

We introduce the definition of the chromatic entropy (Alon & Orlitsky, 1996). A coloring of graph G is the process of assigning colors to vertices such that no adjacent vertices share the same color. Let $\boldsymbol{\pi} = \{\mathbb{C}_1, ..., \mathbb{C}_K\}$ be a coloring with K colors on G, i.e., $\boldsymbol{\pi}$ is a partition of the vertex set V and $\mathbb{C}_k$ is the set of all the vertices with the k-th color class. The entropy of a coloring $\boldsymbol{\pi}$ on a probabilistic graph (G, P) is denoted by $H_c(G, P, \boldsymbol{\pi})$ and is defined as follows.

Definition 2.5 (Entropy of a coloring). Given a probabilistic graph (G, P) with $|V| = n$ and a coloring $\boldsymbol{\pi} = \{\mathbb{C}_1, ..., \mathbb{C}_K\}$, the probability distribution on the coloring $\boldsymbol{\pi}$ is defined by summing up the probability density of the vertices with the same color, i.e,

$$P(\mathbb{C}_k) := \sum_{v \in \mathbb{C}_k} P_v, \ \ \forall k \in \{1, .., K\}, \tag{4}$$

where P_v is the probability density of vertex v. The entropy of a coloring $\boldsymbol{\pi}$ is defined as

$$H_c(G, P, \boldsymbol{\pi}) := \sum_{k=1}^{K} -P(\mathbb{C}_k) \log P(\mathbb{C}_k). \tag{5}$$

Let $\boldsymbol{\Pi}(G)$ be the set of all possible coloring $\boldsymbol{\pi}$ of graph G. Then the chromatic entropy is defined as

Definition 2.6 (Chromatic entropy Alon & Orlitsky (1996)). The chromatic entropy of a probabilistic graph (G, P) is the lowest entropy among all possible colorings of the graph, i.e.,

$$H_\chi(G, P) := \min\{H_c(G, P, \boldsymbol{\pi}) : \boldsymbol{\pi} \in \boldsymbol{\Pi}(G)\}. \tag{6}$$

Let $\chi_H(G, P)$ be the minimum number of colors for $H_\chi(G, P)$ and $\Delta(G)$ be the maximum degree of a vertex in G. It follows that

Corollary 2.7 ((Rezaei, 2013)). $\chi_H(G, P) \leq \Delta(G) + 1$.

2.4 Lower and upper bounds of graph entropy

Let $\alpha(G)$ be the independence number which is the size of the maximum independent set of graph G. The lower bound and upper bound of graph entropy $H_k(G, P)$ are introduced as follows (Boreland, 2018; Alon & Orlitsky, 1996; Cardinal et al., 2004; 2005).

Theorem 2.8 (Lower and upper bounds of graph entropy). *Given a probabilistic graph (G, P), the lower and upper bounds of the graph entropy $H_k(G, P)$ are as follows,*

$$H(P) - \log \alpha(G) \leq H_k(G, P) \leq H_\chi(G, P), \tag{7}$$

where $H(P)$ is the Shannon entropy and $H_\chi(G, P)$ is the chromatic entropy in Definition 2.6.

Corollary 2.9 ((Boreland, 2018)). *The equality of the lower bound in Theorem 2.8 holds if and only if there exists a vector $\boldsymbol{h} \in VP(G)$ satisfying $h_i = P_i\alpha(G)$ for $i = 1, 2, ..., n$.*

Corollary 2.10 ((Rezaei, 2013)). *The equality of the upper bound in Theorem 2.8 holds when G is an empty graph or a complete graph.*

3 Motivation and Problem setup

Our motivation revolves around the utilization of graph entropy as a means to quantify the information contained within graph representations. Specifically, we aim to identify representations that can capture the most significant information, essentially those with the maximum graph entropy. To ensure that node representations accurately capture structural information, we recommend the adoption of orthonormal representations as defined in Definition 2.1. This choice is rooted in the fact that graph entropy can directly serve as a measure of information within orthonormal representations, as indicated by Corollary 2.4. However, an issue arises with the involvement of the probability of each node in Definition 2.3, as it lacks a clear definition. To address this, we introduce the concept of a graph-level representation $\boldsymbol{g}$ and associate a Gaussian distribution P with the vertex set V, using $\boldsymbol{g}$ as the mean. Let $\boldsymbol{Z} = [\mathbf{z}_1, \mathbf{z}_2, \dots, \mathbf{z}_n]$, where $\mathbf{z}_i$ represents the node representation of node i in graph G. We define $P = P(\mathbf{g}, \boldsymbol{Z}) = P1(\mathbf{g}, \boldsymbol{Z}), ..., P_n(\mathbf{g}, \boldsymbol{Z})$, and establish the following:

$$P_i(\mathbf{g}, \boldsymbol{Z}) := \frac{\exp(-\|\boldsymbol{z}_i - \mathbf{g}\|_2^2)}{\sum_{j \in V} \exp(-\|\boldsymbol{z}_j - \mathbf{g}\|_2^2)}, \ \ \forall\, i = 1, 2, ..., n. \tag{8}$$

Then we formulate the learning of orthonormal representation with maximum graph entropy as

$$\max_{\mathbf{g}, \boldsymbol{Z} \in \mathbb{T}(G)} \ \min_{\boldsymbol{a} \in \text{VP}(G)} \sum_{i=1}^{n} -P_i(\mathbf{g}, \boldsymbol{Z}) \log(a_i) \tag{9}$$

Given a set of N graphs $\mathcal{G} = \{G_1, G_2, \dots, G_N\}$ drawn from some unknown distribution $\mathcal{D}$ in $\mathbb{G}$, we want to learn a model $F : \mathbb{G} \to \mathbb{R}^d \times \mathbb{R}^{d \times n}$ to represent each graph as a vector and represent its vertices as vectors, i.e., $(\mathbf{g}_j, \boldsymbol{Z}_j) = F(G_j)$, where F should capture the important information of the underlying distribution $\mathcal{D}$ and $\mathbf{g}_1, \mathbf{g}_2, \dots, \mathbf{g}_N$ should be useful in downstream tasks such as graph classification. Based on (9), we propose to solve the following problem

$$\begin{aligned} &\max_{F \in \mathcal{F}} \ \mathbb{E}_{G \sim \mathcal{D}} \left[\min_{\boldsymbol{a} \in \text{VP}(G)} \sum_{i=1}^{n} -P_i(\mathbf{g}, \boldsymbol{Z}) \log(a_i) \right] \\ &\text{s.t. } (\mathbf{g}, \boldsymbol{Z}) = F(G), \ \boldsymbol{Z} \in \mathbb{T}(G). \end{aligned} \tag{10}$$

The problem equation 10 is our Graph Entropy Maximization (GeMax) problem for graph representation learning.

4 Methodology for Maximizing Graph Entropy.

4.1 Approximation of graph entropy

Directly solving the GeMax problem equation 10 is NP-hard due to the complex vertex packing polytope VP(G) in Definition 2.3. In information theory and combinatorics, graph entropy is typically applied for theoretical analysis rather than practical computation. In this study, we approximate the value of graph entropy using its lower and upper bounds in Theorem 2.8. We can maximize the lower bound of graph entropy $H_k(G, P)$ to estimate the solution of the problem in equation 9, i.e.,

$$\max_{\mathbf{g}, \boldsymbol{Z}} \ H(P(\mathbf{g}, \boldsymbol{Z})) - \log \alpha(G), \ \text{ s.t. } \boldsymbol{Z} \in \mathbb{T}(G). \tag{11}$$

Since the independence number $\alpha(G)$ is a constant of a given G, the optimization in equation 11 is actually learning the orthonormal representations via maximizing the Shannon entropy $H(P(\mathbf{g}, \boldsymbol{Z}))$. Suppose the representations $(\mathbf{g}^*, \boldsymbol{Z}^*)$ yield the maximum of equation 11 where $\boldsymbol{Z}^* \in \mathbb{T}(G)$. Based on Corollary 2.9, if there exists a vector $\boldsymbol{h} \in \text{VP}(G)$ satisfying $h_i = P_i \alpha(G)$ on the vertex set V, the equality of the lower bound in equation 7 holds and we have $H(P(\mathbf{g}^*, \boldsymbol{Z}^*)) - \log \alpha(G) = H_k(G, P(\mathbf{g}^*, \boldsymbol{Z}^*))$. That is, the graph entropy maximization in equation 9 is equivalent to the Shannon entropy maximization equation 11 in this case. However, the equality of the lower bound in equation 7 is not guaranteed to hold for an arbitrary probabilistic graph (G, P). We need to approximate the graph entropy $H_k(G, P)$ for more general cases. According to Theorem 2.8, $H_k(G, P)$ can be represented as a convex combination of the lower and upper bounds as follows.

Corollary 4.1. *There exits $0 \leq \mu \leq 1$ such that*

$$H_k(G, P) = \mu(H(P) - \log \alpha(G)) + (1 - \mu) H_{\chi}(G, P), \tag{12}$$

Given that $\alpha(G)$ is a constant, the orthonormal representations learning problem (9) can be rewritten according to Corollary 4.1 as,

$$\max_{\mathbf{g},\boldsymbol{Z}} \ \mu H(P(\mathbf{g},\boldsymbol{Z})) + (1-\mu)H_{\chi}(G,P(\mathbf{g},\boldsymbol{Z})), \ \text{s.t. } \boldsymbol{Z} \in \mathbb{T}(G), \tag{13}$$

That is, maximizing the graph entropy $H_k(G,P)$ is equivalent to maximizing the Shannon entropy $H(P)$ and chromatic entropy $H_{\chi}(G,P)$ simultaneously. The motivation for maximizing Shannon entropy $H(P)$ is to maximize the lower bound of graph entropy $H_k(G,P)$ in (11). Suppose the coloring $\boldsymbol{\pi}^* = \{\mathbb{C}_1^*, ..., \mathbb{C}_K^*\}$ is the coloring aligns with chromatic entropy $H_{\chi}(G,P)$ where $\mathbb{C}_k^*$ is the set of all nodes in vertex set V with the k-th color. The color set $\mathbb{C}_k^*$ is actually an independent set where the orthonormal representations are orthogonal to each other. Maximizing chromatic entropy $H_{\chi}(G,P)$ is actually to maximize the information contained in independent sets with respect to coloring $\boldsymbol{\pi}^*$. Based on the chromatic entropy Definition 2.6, we reformulate problem (10) as the following constrained max-min problem:

$$\begin{aligned}&\max_{F\in\mathcal{F}} \ \mathbb{E}_{G\sim\mathcal{D}}\left[\min_{\boldsymbol{\pi}} \mu H(P(\mathbf{g},\boldsymbol{Z})) + (1-\mu)H_c(G,P(\mathbf{g},\boldsymbol{Z}),\boldsymbol{\pi})\right]\\ &\quad \text{s.t. } \ (\mathbf{g},\boldsymbol{Z}) = F(G), \ \boldsymbol{Z}\in\mathbb{T}(G), \ \boldsymbol{\pi}\in\boldsymbol{\Pi}(G).\end{aligned} \tag{14}$$

4.2 Representation Learning via GNNs

Parameterization Developing an optimization algorithm to solve the problem 14 is difficult. Thus we learn a GNN model from a set of graphs $\mathcal{G}$ to solve the problem 14 and find the representations of graphs in $\mathcal{G}$. Denote $\mathbb{A}$ as the space of adjacent matrix $\boldsymbol{A}$ and $\mathbb{X}$ as the space of node feature matrix $\boldsymbol{X}$. Let $F_g(\cdot,\cdot;\boldsymbol{\theta}) : \mathbb{A}\times\mathbb{X}\to\mathbb{R}^d$ be a GNN with parameter $\boldsymbol{\theta}$ for graph-level representation learning and $F_Z(\cdot,\cdot;\boldsymbol{\phi}) : \mathbb{A}\times\mathbb{X}\to\mathbb{R}^d$ be another GNN with parameters $\boldsymbol{\phi}$ for node-level representation learning. For $G\in\mathcal{G}$ with adjacency matrix $\boldsymbol{A}$ and feature matrix $\boldsymbol{X}$, we obtain

$$\mathbf{g}^{\theta} = F_g(\boldsymbol{A},\boldsymbol{X};\boldsymbol{\theta}) \ \text{ and } \ \boldsymbol{Z}^{\phi} = F_Z(\boldsymbol{A},\boldsymbol{X};\boldsymbol{\phi}). \tag{15}$$

Let $\boldsymbol{C} = [\boldsymbol{c}_1,...,\boldsymbol{c}_n]^{\top}\in\mathbb{R}^{n\times K}$ be a color probability matrix where $\boldsymbol{c}_i = [c_{i(1)},...,c_{i(K)}]^{\top}$ and $c_{i(k)}$ is the probability of coloring node i with color k, i.e., $i\in\mathbb{C}_k$. According to Corollary 2.7, we can directly set $K = \Delta(G)+1$. Letting $F_c(\cdot,\cdot;\boldsymbol{\psi}) : \mathbb{A}\times\mathbb{X}\to\mathbb{R}^{n\times K}$ be a GNN with parameter $\boldsymbol{\psi}$ for learning coloring, we have

$$\boldsymbol{C}^{\psi} = F_c(\boldsymbol{A},\boldsymbol{X};\boldsymbol{\psi}), \tag{16}$$

where F_c should ensures that $0\le c_{i(k)}^{\psi}\le 1$ and $\sum_{k=1}^{K} c_{i(k)}^{\psi} = 1$. Thus the output activation function of F_c should be a *softmax* function. The coloring $\boldsymbol{\pi}$ can be parameterized by $\boldsymbol{\psi}$ as follows

$$\boldsymbol{\pi}^{\psi} = \{\mathbb{C}_1^{\psi},...,\mathbb{C}_K^{\psi}\} \ \text{ where } \ i\in\mathbb{C}_k^{\psi} \text{ if } k = \underset{q=1,...,K}{\text{argmax}} \ c_{i(q)}^{\psi} \ \ \forall i\in V. \tag{17}$$

Regularizations and Losses Instead of solving constrained optimization, we propose to solve unconstrained optimization with regularization, which is much easier. Based on Definition 2.1, we propose the orthonormal loss $\ell_{\text{orth}}(G;\boldsymbol{\phi})$ for regularization of $\boldsymbol{Z}\in\mathbb{T}(G)$ as follows

$$\ell_{\text{orth}}(G;\boldsymbol{\phi}) = \frac{1}{2}\left\|\left(\boldsymbol{Z}^{\phi}(\boldsymbol{Z}^{\phi})^{\top} - \boldsymbol{I}_n\right)\odot\boldsymbol{M}\right\|_F^2, \tag{18}$$

where $\boldsymbol{M} = \mathbf{1}_{n\times n} - \boldsymbol{A}$ is a binary mask matrix and $\odot$ is the Hadamard product. We also introduce the coloring loss $\ell_{\text{c}}(G;\psi)$ for regularization of $\boldsymbol{\pi}\in\boldsymbol{\Pi}(G)$ as follows

$$\ell_{\text{c}}(G;\boldsymbol{\psi}) = \frac{1}{2}\left\|\left(\boldsymbol{C}^{\psi}(\boldsymbol{C}^{\psi})^{\top}\right)\odot\boldsymbol{A}\right\|_F^2. \tag{19}$$

Therefore, the overall objective function of the regularized rather than the constrained max-min problem 14 on the dataset $\mathcal{G}$ is formulated as

$$\begin{aligned}J(\mathcal{G};\boldsymbol{\theta},\boldsymbol{\phi},\boldsymbol{\psi}) := \sum_{j=1}^{N}\Big\{&\mu H(P(\mathbf{g}_j^{\theta},\boldsymbol{Z}_j^{\phi})) + (1-\mu)H_c(G_j,P(\mathbf{g}_j^{\theta},\boldsymbol{Z}_j^{\phi}),\boldsymbol{\pi}^{\psi})\\ &- \gamma\ell_{\text{orth}}(G_j;\boldsymbol{\phi}) + \eta\ell_{\text{c}}(G_j;\boldsymbol{\psi})\Big\},\end{aligned} \tag{20}$$

where γ and η are positive hyperparameters for regularization.

Iterative Optimization Given a coloring $\boldsymbol{\pi}^*$, the representations updating sub-problem is to optimize $\boldsymbol{\theta}$ and $\boldsymbol{\phi}$ with a fixed $\boldsymbol{\psi}^*$ as follows

$$\theta^*, \phi^* = \underset{\theta,\phi}{\operatorname{argmax}}\, J(\mathcal{G}; \boldsymbol{\theta}, \boldsymbol{\phi}, \boldsymbol{\psi}^*), \tag{21}$$

Given graph representations $(\mathbf{g}^*, \boldsymbol{Z}^*)$, the coloring updating sub-problem is to optimize $\boldsymbol{\psi}$ with fixed $\boldsymbol{\theta}^*$ and $\boldsymbol{\phi}^*$ as follows

$$\boldsymbol{\psi}^* = \underset{\boldsymbol{\psi}}{\operatorname{argmin}}\, J(\mathcal{G}; \boldsymbol{\theta}^*, \boldsymbol{\phi}^*, \boldsymbol{\psi}), \tag{22}$$

It is worth noting that we have relaxed the original constrained optimization to a regularized unconstrained optimization. The solution cannot satisfy the constraints exactly. To ensure the constraints, one may consider using the exact penalty method to solve the problem, which is just increasing γ and η gradually in the iterative optimization. But we have found that the representations given the regularized optimization are as good as those given by the constrained optimization. The comparison experiments between regularized and constrained optimization are in Appendix A.11.

Error Bound Let $\hat{\mu}$ be an estimator of μ and $\hat{H}_k(G,P)$ be the approximation of $H_k(G,P)$ with respect to $\hat{\mu}$. Let δ be the upper bound of error bound of our approximation. Let $\chi(G)$ be chromatic number of graph G which is the smallest number of colors needed to color the vertices.

Corollary 4.2. *Let* $\epsilon = \frac{\log \chi(G)}{1+\delta} + \log \alpha(G)$, *if* $H(P) \geq \epsilon$, *we have* $\frac{|H_k(G,P) - \hat{H}_k(G,P)|}{H_k(G,P)} \leq \delta$.

This means that if the Shannon entropy is larger than ϵ, the error bound of approximation is less than δ. The proof of Corollary 4.2 is in Appendix A.2. In the t iteration, the average Shannon entropy of the dataset $\mathcal{G}$ is defined as

$$\bar{H}(\mathcal{G}; t) := \frac{1}{N} \sum_{j=1}^{N} H(P({\mathbf{g}_j}^{\theta^t}, {\boldsymbol{Z}_j}^{\phi^t})). \tag{23}$$

Based on Corollary 4.2, if $\bar{H}(\mathcal{G}; t) < \epsilon$ and $\mu^t + 0.01 \leq 1$, we use $\mu^{t+1} = \mu^t + 0.01$ to increase the average Shannon entropy of $\mathcal{G}$ for a more exact approximation.

Algorithm 1 Iterative algorithm for solving the regularized max-min problem (14)

```
Initialization: $\boldsymbol{\theta}^0, \boldsymbol{\phi}^0, \boldsymbol{\psi}^0, \mu^0 = 0.5, \gamma = 0.5, \eta = 0.5, \epsilon$ (e.g., $0.3 \log n$), $\varepsilon$ (e.g., 0.01).
repeat
    $\theta^{t+1}, \phi^{t+1} = \operatorname{argmax}_{\theta,\phi} J(\mathcal{G}; \boldsymbol{\theta}, \boldsymbol{\phi}, \boldsymbol{\psi}^t)$
    $\boldsymbol{\psi}^{t+1} = \operatorname{argmin}_{\boldsymbol{\psi}} J(\mathcal{G}; \boldsymbol{\theta}^{t+1}, \boldsymbol{\phi}^{t+1}, \boldsymbol{\psi})$
    if $\bar{H}(\mathcal{G}; t) < \epsilon$ and $\mu^t + 0.01 \leq 1$ then $\mu^{t+1} = \mu^t + 0.01$ else $\mu^{t+1} = \mu^t$
until $|J(\mathcal{G}; \boldsymbol{\theta}^{t+1}, \boldsymbol{\phi}^{t+1}, \boldsymbol{\psi}^{t+1}) - J(\mathcal{G}; \boldsymbol{\theta}^t, \boldsymbol{\phi}^t, \boldsymbol{\psi}^t)| \leq \varepsilon$
```

4.3 Architecture and Generalizations

The architecture of our GeMax method is in Figure 2 of Appendix A.3. The graph representations learning functions $F_g(\cdot, \cdot; \boldsymbol{\theta})$ and $F_Z(\cdot, \cdot; \boldsymbol{\phi})$ are not confined to any specific GNN models or graph data; rather, it offers a versatile approach across various contexts. For example, we can use one of the InfoMax-based models (e.g. InfoGraph (Sun et al., 2019) or GraphCL (You et al., 2020)) to model graph representation learning F_g and F_Z for our GeMax (see Figure 3 in Appendix A.3). In conclusion, our graph entropy maximization principle is parallel to other unsupervised graph learning principles such as InfoMax principle (Linsker, 1988).

5 Experiment

In this section, we will evaluate the effectiveness of our Graph entropy Maximization (GeMax) method on graph-level and node-level tasks. The statistics of graph datasets used in experiments are in Table 6 and Table 7 of Appendix A.4. In Appendix A.5, we introduce our main baseline InfoMax (Linsker, 1988). We provide the experimental settings of node-level learning in Appendix

A.7. In Appendix A.8, we conduct sensitivity analysis on all the hyperparameters and provide some recommendations for parameter settings. In Appendix A.9, we conduct an ablation study to analyze the importance of each part in our graph entropy maximization methods. In Appendix A.10, we analyze the convergence of our iterative algorithm 1. In Appendix A.11, we compare the regularized and constrained optimization of problem equation 14. In Appendix A.12, we report the time cost of our methods on different tasks and datasets.

5.1 GRAPH-LEVEL REPRESENTATIONS LEARNING

For unsupervised graph-level learning, those InfoMax based methods are the most current and influential methods spanning from 2019 to 2022, each boasting high citations on Google Scholar (see Table 8). Besides InfoMax, there are few works on other graph-level representation learning principles such as graph information bottleneck (GIB) Wu et al. (2020) and the subgraph information bottleneck (SIB) Yu et al. (2021). But they are not suitable for unsupervised graph learning (see Appendix A.5). To ensure fair comparisons, we follow the neural network architectures of InfoMax methods and replace the InfoMax objective with our GeMax objective in equation 20. Our baselines include three kernel methods (e.g. graphlet kernel (GL) (Shervashidze et al., 2009), Weisfeiler-Lehman sub-tree kernel (WL) (Shervashidze et al., 2011), deep graph kernel (DGK) (Yanardag & Vishwanathan, 2015)), two traditional graph embedding methods (e.g. node2vec (Grover & Leskovec, 2016), and graph2vec (Narayanan et al., 2017)), and five InfoMax based methods (e.g InfoGraph (Sun et al., 2019), GraphCL (You et al., 2020), AD-GCL (Suresh et al., 2021), JOAO (You et al., 2021), AutoGCL (Yin et al., 2022)).

Unsupervised learning Following (Sun et al., 2019; You et al., 2021; Yin et al., 2022), we train a graph representation model on unlabeled data to obtain graph representations and use these representations and graph labels to train a SVM classifier. Our experimental setup follows AutoGCL (Yin et al., 2022). Specifically, they use a 5-layer GIN Xu et al. (2018) with hidden size 128 as the representation model, shown in Figure 4. The model is trained with a batch size of 128 and a learning rate of 0.001. For those contrastive learning methods (e.g., JOJOv2 and AutoGCL), they use 30 epochs of contrastive pre-training under the naive strategy. We repeat the experiments for 10 times with different random seeds. In each time, we perform 10-fold cross-validation on each dataset. The hyperparameters of Algorithm 1 are $\mu^0 = 0.5, \gamma = 0.5, \eta = 0.5, \epsilon = 0.3 \log n, \tau = 0.01$. We also conduct sensitivity analysis in Appendix A.8 to study how different hyperparameters affect the results. The results are reported in Table 14.

Semi-supervised Learning Following (Hu et al., 2019; You et al., 2021; Yin et al., 2022), we compare our GeMax methods with InfoMax-based methods in semi-supervised learning tasks. The semi-supervised learning objective of InfoMax method is shown in equation 29 of Appendix A.5. To ensure fair comparisons, we replace the InfoMax objective with our GeMax objective in equation 20 while keeping other settings unchanged. Following the settings of AutoGCL (Yin et al., 2022), we employ a 10-fold cross-validation on each dataset. For each fold, we use 80% of the total data as the unlabeled data, 10% as labeled training data, and 10% as labeled testing data. The classifier for labeled data is a ResGCN (Chen et al., 2019) with 5 layers and a hidden size of 128. The hyperparameters of Algorithm 1 are $\mu^0 = 0.5, \gamma = 0.5, \eta = 0.5, \epsilon = 0.3 \log n, \tau = 0.01$. We repeat each experiment 10 times and report the average accuracy in Table 2.

Significance analysis Our GeMax method achieves the best performance on all datasets. By replacing the InfoMax objective with GeMax objective, the performance of the five graph representation learning methods can be improved, which demonstrates the effectiveness of our GeMax method. we apply the paired t-test on the mean scores over the datasets to show the significance of our improvement over baselines. A p-value less than 0.05 indicates a significant difference. The results in Table 3 demonstrates the significance of gains given by our methods.

5.2 UNSUPREVISED NODE-LEVEL LEARNING

As mentioned above, the orthonormal representations can be used for graph reconstruction. We compare GeMax methods with VGAE Kipf & Welling (2016b), ARGA Pan et al. (2018), GIC Mavromatis & Karypis (2020) and LGAE Salha et al. (2021) in edge prediction tasks. Following

Table 1: Performance (ACC) of unsupervised learning. The baseline results are from AutoGCL (Yin et al., 2022) and JOAO (You et al., 2021). The **bold**, blue and green numbers denote the best, second best and third best performances respectively, which also applies to Table 2 and Table 4

methods and principles		MUTAG	PROTEINS	DD	NCI1	COLLAB	IMDB-B	REDDIT-B	REDDIT-M5K
kernels	GL	81.66±2.11	-	-	-	-	65.87±0.98	77.34±0.18	41.01± 0.17
	WL	80.72±3.00	72.92±0.56	-	80.01±0.50	-	72.30±3.44	68.82±0.41	46.06± 0.21
	DGK	87.44±2.72	73.30±0.82	-	80.31±0.46	-	66.96±0.56	78.04±0.39	41.27±0.18
vector embedding	node2vec	72.63±10.20	57.49±3.57	-	54.89±1.61	-	-	-	-
	graph2vec	83.15±9.25	73.30±2.05	-	73.22±1.81	-	71.10±0.54	75.78±1.03	47.86±0.26
InfoGraph	InfoMax	89.01±1.13	74.44±0.31	72.85±1.78	76.20±1.06	70.65±1.13	73.03±0.87	82.50±1.42	53.46±1.03
	GeMax	**91.13±1.70**	75.77±1.26	74.16±1.65	79.24±1.43	72.57±1.74	**74.59±1.53**	85.53±1.92	55.21±1.69
GraphCL	InfoMax	86.80±1.34	74.39±0.45	78.62±0.40	77.87±0.41	71.36±1.15	71.14±0.44	89.53±0.84	55.99±0.28
	GeMax	90.36±1.69	**76.86±1.62**	**79.25±1.53**	78.72±1.79	73.43±1.62	73.12±1.25	**91.47±1.74**	56.25±1.53
AD-GCL	InfoMax	87.13±1.56	73.59±0.65	74.49±0.52	69.67±0.51	73.32±0.61	71.57±1.01	85.52±0.79	53.00±0.82
	GeMax	89.68±1.47	74.52±1.71	77.58±1.41	76.35±1.62	**74.83±1.79**	73.52±1.45	88.03±1.62	55.03±1.54
JOAOv2	InfoMax	86.91±1.01	71.25±0.85	66.91±1.75	72.99±0.75	70.40±2.21	71.60±0.86	78.35±1.38	55.57±2.86
	GeMax	88.33±1.58	74.63±1.87	72.60±1.35	75.36±1.42	71.68±1.67	72.21±1.72	81.68±1.40	**57.17±1.67**
AutoGCL	InfoMax	88.64±1.08	75.80±0.36	77.57±0.60	82.00±0.29	70.12±0.68	73.30±0.40	88.58±1.49	56.75±0.18
	GeMax	90.85±1.28	76.23±1.29	78.36±1.51	**83.21±1.34**	72.39±1.57	74.05±1.79	90.42±1.31	56.81±1.85

Table 2: Performance (ACC) of semi-supervised learning.

	methods	NCI1	PROTEINS	DD	COLLAB	REDDIT-B	REDDIT-M5K	GITHUB
GraphCL	InfoMax	74.63±0.25	74.17±0.34	76.17±1.37	74.23±0.21	89.11±0.19	52.55±0.45	65.81±0.79
	GeMax	75.49±1.76	75.39±1.58	77.61±1.29	76.57±1.72	**91.45±1.57**	54.61±1.70	66.78±1.53
AD-GCL	InfoMax	75.18±0.31	73.96±0.47	77.91±0.73	75.82±0.26	90.10±0.15	53.49±0.28	64.17±1.38
	GeMax	76.27±1.44	75.21±1.78	**78.52±1.53**	76.92±1.81	91.32±1.67	**54.88±1.21**	65.52±1.45
JOAOv2	InfoMax	74.86±0.39	73.31±0.48	75.81±0.72	75.53±0.18	88.79±0.65	52.71±0.28	66.66±0.60
	GeMax	**76.05±1.23**	74.52±1.61	76.30±1.54	76.25±1.24	90.05±1.76	54.07±1.52	66.47±1.93
AutoGCL	InfoMax	73.75±2.25	75.65±2.40	77.50±4.41	77.16±1.48	79.80±3.47	49.91±2.70	62.46±1.51
	GeMax	75.12±1.19	**76.75±1.83**	78.36±1.37	**78.93±1.80**	87.26±1.68	52.76±1.74	**67.31±1.64**

Table 3: Significance analysis of improvement. We report the p-values of paired t-test.

task (principles)	InfoGraph	GraphCL	AD-GCL	JOAOv2	AutoGCL
unsupervised (InfoMax vs GeMax)	0.0005	0.0029	0.0036	0.0037	0.0047
semi-supervised (InfoMax vs GeMax)	-	0.0005	0.0000	0.0067	0.0200

VGAE Kipf & Welling (2016b), all the models are trained on an incomplete version of these datasets where parts of the edges have been removed, while all node features are kept. We split the nodes of each dataset into three parts: 80% as training set, 10% as validation set and 10% as test set. We set γ larger to emphasize the orthonormal representations regularization. The hyperparameters of Algorithm 1 are $\mu^0 = 0.5, \gamma = 5, \eta = 0.5, \epsilon = 0.3 \log n, \tau = 0.01$. The results in Table 4 show that GeMax methods outperform baselines.

Table 4: Performance of edge prediction. AUC is the area under ROC curve. AP is average precision.

methods	Cora		Citeseer		Pubmed	
	AUC	AP	AUC	AP	AUC	AP
VGAE	91.4±0.16	92.6±0.10	90.8±0.07	92.3±0.11	94.5±0.13	94.8±0.09
ARGA	92.3±0.21	92.5±0.13	93.1±0.16	93.5±0.25	96.3±0.26	96.8±0.15
LGAE	93.0±0.19	93.2±0.08	94.5±0.19	94.7±0.12	96.7±0.15	97.0±0.18
GIC	92.6±0.09	92.7±0.17	94.3±0.23	94.4±0.14	96.5±0.17	96.7±0.21
InfoGraph-GeMax	92.8±0.13	93.0±0.25	93.7±0.12	94.2±0.17	95.2±0.24	95.4±0.12
GraphCL-GeMax	**93.2±0.24**	**93.4±0.19**	94.6±0.20	94.9±0.23	96.6±0.13	96.7±0.10
AutoGCL-GeMax	93.1±0.15	93.2±0.21	**94.9±0.14**	**95.1±0.13**	**96.9±0.19**	**97.2±0.15**

5.3 More Numerical Results

The results of **parameter sensitivity analysis**, **ablation study**, **convergence analysis** and **time cost** are in the supplementary material.

6 Conclusions

In this work, we propose a novel Graph entropy Maximization (GeMax) method to learn the orthonormal representations, which can capture the most information of a graph. We also approximate the graph entropy via Shannon entropy and chromatic entropy. The experiment on unsupervised graph-level and node-level demenstrate the effectiveness of our GeMax method.

REFERENCES

Noga Alon and Alon Orlitsky. Source coding and graph entropies. *IEEE Transactions on Information Theory*, 42(5):1329–1339, 1996.

Furqan Aziz, Edwin R Hancock, and Richard C Wilson. Network entropy using edge-based information functionals. *Journal of Complex Networks*, 8(3):cnaa015, 2020.

Yunsheng Bai, Hao Ding, Yang Qiao, Agustin Marinovic, Ken Gu, Ting Chen, Yizhou Sun, and Wei Wang. Unsupervised inductive graph-level representation learning via graph-graph proximity. *arXiv preprint arXiv:1904.01098*, 2019.

Mohamed Ishmael Belghazi, Aristide Baratin, Sai Rajeshwar, Sherjil Ozair, Yoshua Bengio, Aaron Courville, and Devon Hjelm. Mutual information neural estimation. In *International conference on machine learning*, pp. 531–540. PMLR, 2018.

Gareth Boreland. A lower bound on graph entropy. In *Mathematical Proceedings of the Royal Irish Academy*, volume 118, pp. 9–20. Royal Irish Academy, 2018.

Karsten M Borgwardt, Cheng Soon Ong, Stefan Schönauer, SVN Vishwanathan, Alex J Smola, and Hans-Peter Kriegel. Protein function prediction via graph kernels. *Bioinformatics*, 21(suppl_1): i47–i56, 2005.

Bernadette Bouchon, Lorenza Saitta, and Ronald R Yager. *Uncertainty and Intelligent Systems: 2nd International Conference on Information Processing and Management of Uncertainty in Knowledge Based Systems IPMU'88. Urbino, Italy, July 4-7, 1988. Proceedings*, volume 313. Springer Science & Business Media, 1988.

Jean Cardinal, Samuel Fiorini, and Gilles Van Assche. On minimum entropy graph colorings. In *International Symposium onInformation Theory, 2004. ISIT 2004. Proceedings.*, pp. 43. IEEE, 2004.

Jean Cardinal, Samuel Fiorini, and Gwenaël Joret. Minimum entropy coloring. In *International Symposium on Algorithms and Computation*, pp. 819–828. Springer, 2005.

Ting Chen, Song Bian, and Yizhou Sun. Are powerful graph neural nets necessary? a dissection on graph classification. *arXiv preprint arXiv:1905.04579*, 2019.

Ganqu Cui, Jie Zhou, Cheng Yang, and Zhiyuan Liu. Adaptive graph encoder for attributed graph embedding. In *Proceedings of the 26th ACM SIGKDD International Conference on Knowledge Discovery & Data Mining*, pp. 976–985, 2020.

Asim Kumar Debnath, Rosa L Lopez de Compadre, Gargi Debnath, Alan J Shusterman, and Corwin Hansch. Structure-activity relationship of mutagenic aromatic and heteroaromatic nitro compounds. correlation with molecular orbital energies and hydrophobicity. *Journal of medicinal chemistry*, 34(2):786–797, 1991.

Matthias Dehmer. Information processing in complex networks: Graph entropy and information functionals. *Applied Mathematics and Computation*, 201(1-2):82–94, 2008.

Matthias Dehmer and Abbe Mowshowitz. A history of graph entropy measures. *Information Sciences*, 181(1):57–78, 2011.

Kaize Ding, Zhe Xu, Hanghang Tong, and Huan Liu. Data augmentation for deep graph learning: A survey. *ACM SIGKDD Explorations Newsletter*, 24(2):61–77, 2022.

Kaize Ding, Yancheng Wang, Yingzhen Yang, and Huan Liu. Eliciting structural and semantic global knowledge in unsupervised graph contrastive learning. In *Proceedings of the AAAI Conference on Artificial Intelligence*, volume 37, pp. 7378–7386, 2023.

Minjing Dong, Hanting Chen, Yunhe Wang, and Chang Xu. Crafting efficient neural graph of large entropy. In *IJCAI*, pp. 2244–2250, 2019.

Jingcan Duan, Siwei Wang, Pei Zhang, En Zhu, Jingtao Hu, Hu Jin, Yue Liu, and Zhibin Dong. Graph anomaly detection via multi-scale contrastive learning networks with augmented view. In *Proceedings of the AAAI Conference on Artificial Intelligence*, volume 37, pp. 7459–7467, 2023.

Peng Fang, Fang Wang, Zhan Shi, Hong Jiang, Dan Feng, and Lei Yang. Huge: An entropy-driven approach to efficient and scalable graph embeddings. In *2021 IEEE 37th International Conference on Data Engineering (ICDE)*, pp. 2045–2050. IEEE, 2021.

Yin Fang, Qiang Zhang, Haihong Yang, Xiang Zhuang, Shumin Deng, Wen Zhang, Ming Qin, Zhuo Chen, Xiaohui Fan, and Huajun Chen. Molecular contrastive learning with chemical element knowledge graph. In *Proceedings of the AAAI Conference on Artificial Intelligence*, volume 36, pp. 3968–3976, 2022.

Bent Fuglede and Flemming Topsoe. Jensen-shannon divergence and hilbert space embedding. In *International symposium onInformation theory, 2004. ISIT 2004. Proceedings.*, pp. 31. IEEE, 2004.

Justin Gilmer, Samuel S Schoenholz, Patrick F Riley, Oriol Vinyals, and George E Dahl. Neural message passing for quantum chemistry. In *International conference on machine learning*, pp. 1263–1272. PMLR, 2017.

Maria Grebenkina, Anselm Brachmann, Marco Bertamini, Ali Kaduhm, and Christoph Redies. Edge-orientation entropy predicts preference for diverse types of man-made images. *Frontiers in Neuroscience*, 12:678, 2018.

Aditya Grover and Jure Leskovec. node2vec: Scalable feature learning for networks. In *Proceedings of the 22nd ACM SIGKDD international conference on Knowledge discovery and data mining*, pp. 855–864, 2016.

Will Hamilton, Zhitao Ying, and Jure Leskovec. Inductive representation learning on large graphs. *Advances in neural information processing systems*, 30, 2017a.

William L Hamilton, Rex Ying, and Jure Leskovec. Representation learning on graphs: Methods and applications. *arXiv preprint arXiv:1709.05584*, 2017b.

Xiaotian Han, Zhimeng Jiang, Ninghao Liu, and Xia Hu. G-mixup: Graph data augmentation for graph classification. In *International Conference on Machine Learning*, pp. 8230–8248. PMLR, 2022.

R Devon Hjelm, Alex Fedorov, Samuel Lavoie-Marchildon, Karan Grewal, Phil Bachman, Adam Trischler, and Yoshua Bengio. Learning deep representations by mutual information estimation and maximization. In *International Conference on Learning Representations*, 2019.

Zhenyu Hou, Xiao Liu, Yukuo Cen, Yuxiao Dong, Hongxia Yang, Chunjie Wang, and Jie Tang. Graphmae: Self-supervised masked graph autoencoders. In *Proceedings of the 28th ACM SIGKDD Conference on Knowledge Discovery and Data Mining*, pp. 594–604, 2022.

Weihua Hu, Bowen Liu, Joseph Gomes, Marinka Zitnik, Percy Liang, Vijay Pande, and Jure Leskovec. Strategies for pre-training graph neural networks. *arXiv preprint arXiv:1905.12265*, 2019.

Lavender Y Jiang, John Shi, Mark Cheung, Oren Wright, and José MF Moura. Edge entropy as an indicator of the effectiveness of gnns over cnns for node classification. In *2020 54th Asilomar Conference on Signals, Systems, and Computers*, pp. 746–750. IEEE, 2020.

Thomas Kipf, Ethan Fetaya, Kuan-Chieh Wang, Max Welling, and Richard Zemel. Neural relational inference for interacting systems. In *International Conference on Machine Learning*, pp. 2688–2697. PMLR, 2018.

Thomas N Kipf and Max Welling. Semi-supervised classification with graph convolutional networks. *arXiv preprint arXiv:1609.02907*, 2016a.

Thomas N Kipf and Max Welling. Variational graph auto-encoders. *arXiv preprint arXiv:1611.07308*, 2016b.

János Körner. Coding of an information source having ambiguous alphabet and the entropy of graphs. In *6th Prague conference on information theory*, pp. 411–425, 1973.

Nils Kriege and Petra Mutzel. Subgraph matching kernels for attributed graphs. *arXiv preprint arXiv:1206.6483*, 2012.

Phuc H Le-Khac, Graham Healy, and Alan F Smeaton. Contrastive representation learning: A framework and review. *Ieee Access*, 8:193907–193934, 2020.

Namkyeong Lee, Junseok Lee, and Chanyoung Park. Augmentation-free self-supervised learning on graphs. In *Proceedings of the AAAI Conference on Artificial Intelligence*, volume 36, pp. 7372–7380, 2022.

Shuangli Li, Jingbo Zhou, Tong Xu, Dejing Dou, and Hui Xiong. Geomgcl: Geometric graph contrastive learning for molecular property prediction. In *Proceedings of the AAAI Conference on Artificial Intelligence*, volume 36, pp. 4541–4549, 2022a.

Yinqi Li, Hong Chang, Bingpeng Ma, Shiguang Shan, and Xilin Chen. Optimal positive generation via latent transformation for contrastive learning. *Advances in Neural Information Processing Systems*, 35:18327–18342, 2022b.

Ralph Linsker. Self-organization in a perceptual network. *Computer*, 21(3):105–117, 1988.

Xuecheng Liu, Luoyi Fu, and Xinbing Wang. Bridging the gap between von neumann graph entropy and structural information: Theory and applications. In *Proceedings of the Web Conference 2021*, pp. 3699–3710, 2021.

Xuecheng Liu, Luoyi Fu, Xinbing Wang, and Chenghu Zhou. On the similarity between von neumann graph entropy and structural information: Interpretation, computation, and applications. *IEEE Transactions on Information Theory*, 68(4):2182–2202, 2022a.

Yixin Liu, Ming Jin, Shirui Pan, Chuan Zhou, Yu Zheng, Feng Xia, and S Yu Philip. Graph self-supervised learning: A survey. *IEEE Transactions on Knowledge and Data Engineering*, 35(6): 5879–5900, 2022b.

László Lovász. On the shannon capacity of a graph. *IEEE Transactions on Information theory*, 25 (1):1–7, 1979.

Gongxu Luo, Jianxin Li, Jianlin Su, Hao Peng, Carl Yang, Lichao Sun, Philip S Yu, and Lifang He. Graph entropy guided node embedding dimension selection for graph neural networks. *arXiv preprint arXiv:2105.03178*, 2021.

Xiao Luo, Wei Ju, Yiyang Gu, Zhengyang Mao, Luchen Liu, Yuhui Yuan, and Ming Zhang. Self-supervised graph-level representation learning with adversarial contrastive learning. *ACM Transactions on Knowledge Discovery from Data*, 2023a.

Yi Luo, Guangchun Luo, Ke Qin, and Aiguo Chen. Graph entropy minimization for semi-supervised node classification, 2023b.

Yixuan Ma, Xiaolin Zhang, Peng Zhang, and Kun Zhan. Entropy neural estimation for graph contrastive learning. In *Proceedings of the 31st ACM International Conference on Multimedia*, pp. 435–443, 2023.

Costas Mavromatis and George Karypis. Graph infoclust: Leveraging cluster-level node information for unsupervised graph representation learning. *arXiv preprint arXiv:2009.06946*, 2020.

Giorgia Minello, Luca Rossi, and Andrea Torsello. On the von neumann entropy of graphs. *Journal of Complex Networks*, 7(4):491–514, 2019.

Yujie Mo, Liang Peng, Jie Xu, Xiaoshuang Shi, and Xiaofeng Zhu. Simple unsupervised graph representation learning. In *Proceedings of the AAAI Conference on Artificial Intelligence*, volume 36, pp. 7797–7805, 2022.

Christopher Morris, Nils M. Kriege, Franka Bause, Kristian Kersting, Petra Mutzel, and Marion Neumann. Tudataset: A collection of benchmark datasets for learning with graphs. In *ICML 2020 Workshop on Graph Representation Learning and Beyond (GRL+ 2020)*, 2020. URL www.graphlearning.io.

Abbe Mowshowitz and Matthias Dehmer. Entropy and the complexity of graphs revisited. *Entropy*, 14(3):559–570, 2012.

Annamalai Narayanan, Mahinthan Chandramohan, Rajasekar Venkatesan, Lihui Chen, Yang Liu, and Shantanu Jaiswal. graph2vec: Learning distributed representations of graphs. *arXiv preprint arXiv:1707.05005*, 2017.

Sebastian Nowozin, Botond Cseke, and Ryota Tomioka. f-gan: Training generative neural samplers using variational divergence minimization. *Advances in neural information processing systems*, 29, 2016.

Frédérique Oggier and Anwitaman Datta. Renyi entropy driven hierarchical graph clustering. *PeerJ Computer Science*, 7:e366, 2021.

Dávid Pál, Barnabás Póczos, and Csaba Szepesvári. Estimation of rényi entropy and mutual information based on generalized nearest-neighbor graphs. *Advances in Neural Information Processing Systems*, 23, 2010.

Shirui Pan, Ruiqi Hu, Guodong Long, Jing Jiang, Lina Yao, and Chengqi Zhang. Adversarially regularized graph autoencoder for graph embedding. *arXiv preprint arXiv:1802.04407*, 2018.

Filippo Passerini and Simone Severini. The von neumann entropy of networks. *arXiv preprint arXiv:0812.2597*, 2008.

Jiezhong Qiu, Qibin Chen, Yuxiao Dong, Jing Zhang, Hongxia Yang, Ming Ding, Kuansan Wang, and Jie Tang. Gcc: Graph contrastive coding for graph neural network pre-training. In *Proceedings of the 26th ACM SIGKDD international conference on knowledge discovery & data mining*, pp. 1150–1160, 2020.

Seyed Saeed Changiz Rezaei. Entropy and graphs. *arXiv preprint arXiv:1311.5632*, 2013.

Yu Rong, Yatao Bian, Tingyang Xu, Weiyang Xie, Ying Wei, Wenbing Huang, and Junzhou Huang. Self-supervised graph transformer on large-scale molecular data. *Advances in Neural Information Processing Systems*, 33:12559–12571, 2020.

Guillaume Salha, Romain Hennequin, and Michalis Vazirgiannis. Simple and effective graph autoencoders with one-hop linear models. In *Machine Learning and Knowledge Discovery in Databases: European Conference, ECML PKDD 2020, Ghent, Belgium, September 14–18, 2020, Proceedings, Part I*, pp. 319–334. Springer, 2021.

Prithviraj Sen, Galileo Namata, Mustafa Bilgic, Lise Getoor, Brian Galligher, and Tina Eliassi-Rad. Collective classification in network data. *AI magazine*, 29(3):93–93, 2008.

Claude Elwood Shannon. A mathematical theory of communication. *The Bell system technical journal*, 27(3):379–423, 1948.

Xiao Shen, Dewang Sun, Shirui Pan, Xi Zhou, and Laurence T Yang. Neighbor contrastive learning on learnable graph augmentation. In *Proceedings of the AAAI Conference on Artificial Intelligence*, volume 37, pp. 9782–9791, 2023.

Nino Shervashidze, SVN Vishwanathan, Tobias Petri, Kurt Mehlhorn, and Karsten Borgwardt. Efficient graphlet kernels for large graph comparison. In *Artificial intelligence and statistics*, pp. 488–495. PMLR, 2009.

Nino Shervashidze, Pascal Schweitzer, Erik Jan Van Leeuwen, Kurt Mehlhorn, and Karsten M Borgwardt. Weisfeiler-lehman graph kernels. *Journal of Machine Learning Research*, 12(9), 2011.

Fan-Yun Sun, Jordan Hoffmann, Vikas Verma, and Jian Tang. Infograph: Unsupervised and semi-supervised graph-level representation learning via mutual information maximization. *arXiv preprint arXiv:1908.01000*, 2019.

Ziheng Sun, Chris Ding, and Jicong Fan. Lovász principle for unsupervised graph representation learning. In *Thirty-seventh Conference on Neural Information Processing Systems*, 2023.

Susheel Suresh, Pan Li, Cong Hao, and Jennifer Neville. Adversarial graph augmentation to improve graph contrastive learning. *Advances in Neural Information Processing Systems*, 34:15920–15933, 2021.

Puja Trivedi, Ekdeep Singh Lubana, Yujun Yan, Yaoqing Yang, and Danai Koutra. Augmentations in graph contrastive learning: Current methodological flaws & towards better practices. In *Proceedings of the ACM Web Conference 2022*, pp. 1538–1549, 2022.

Petar Veličković, Guillem Cucurull, Arantxa Casanova, Adriana Romero, Pietro Lio, and Yoshua Bengio. Graph attention networks. *arXiv preprint arXiv:1710.10903*, 2017.

Saurabh Verma and Zhi-Li Zhang. Learning universal graph neural network embeddings with aid of transfer learning. *arXiv preprint arXiv:1909.10086*, 2019.

Jianjia Wang, Richard C Wilson, and Edwin R Hancock. Network edge entropy decomposition with spin statistics. *Pattern Recognition*, 118:108040, 2021.

Yifei Wang, Yupan Wang, Zeyu Zhang, Song Yang, Kaiqi Zhao, and Jiamou Liu. User: Unsupervised structural entropy-based robust graph neural network. *arXiv preprint arXiv:2302.05889*, 2023.

Chunyu Wei, Jian Liang, Di Liu, and Fei Wang. Contrastive graph structure learning via information bottleneck for recommendation. *Advances in Neural Information Processing Systems*, 35:20407–20420, 2022.

Chunyu Wei, Yu Wang, Bing Bai, Kai Ni, David Brady, and Lu Fang. Boosting graph contrastive learning via graph contrastive saliency. In *International conference on machine learning*, pp. 36839–36855. PMLR, 2023.

Jiancan Wu, Xiang Wang, Fuli Feng, Xiangnan He, Liang Chen, Jianxun Lian, and Xing Xie. Self-supervised graph learning for recommendation. In *Proceedings of the 44th international ACM SIGIR conference on research and development in information retrieval*, pp. 726–735, 2021.

Junran Wu, Xueyuan Chen, Ke Xu, and Shangzhe Li. Structural entropy guided graph hierarchical pooling. In *International conference on machine learning*, pp. 24017–24030. PMLR, 2022.

Tailin Wu, Hongyu Ren, Pan Li, and Jure Leskovec. Graph information bottleneck. *Advances in Neural Information Processing Systems*, 33:20437–20448, 2020.

Jun Xia, Lirong Wu, Jintao Chen, Bozhen Hu, and Stan Z Li. Simgrace: A simple framework for graph contrastive learning without data augmentation. In *Proceedings of the ACM Web Conference 2022*, pp. 1070–1079, 2022.

Teng Xiao, Zhengyu Chen, Zhimeng Guo, Zeyang Zhuang, and Suhang Wang. Decoupled self-supervised learning for graphs. *Advances in Neural Information Processing Systems*, 35:620–634, 2022.

Tian Xie and Jeffrey C Grossman. Crystal graph convolutional neural networks for an accurate and interpretable prediction of material properties. *Physical review letters*, 120(14):145301, 2018.

Yaochen Xie, Zhao Xu, Jingtun Zhang, Zhengyang Wang, and Shuiwang Ji. Self-supervised learning of graph neural networks: A unified review. *IEEE transactions on pattern analysis and machine intelligence*, 2022.

Dongkuan Xu, Wei Cheng, Dongsheng Luo, Haifeng Chen, and Xiang Zhang. Infogcl: Information-aware graph contrastive learning. *Advances in Neural Information Processing Systems*, 34:30414–30425, 2021.

Keyulu Xu, Weihua Hu, Jure Leskovec, and Stefanie Jegelka. How powerful are graph neural networks? *arXiv preprint arXiv:1810.00826*, 2018.

Pinar Yanardag and SVN Vishwanathan. Deep graph kernels. In *Proceedings of the 21th ACM SIGKDD international conference on knowledge discovery and data mining*, pp. 1365–1374, 2015.

Zhenyu Yang, Ge Zhang, Jia Wu, Jian Yang, Quan Z Sheng, Hao Peng, Angsheng Li, Shan Xue, and Jianlin Su. Minimum entropy principle guided graph neural networks. In *Proceedings of the Sixteenth ACM International Conference on Web Search and Data Mining*, pp. 114–122, 2023.

Cheng Ye, Richard C Wilson, César H Comin, Luciano da F Costa, and Edwin R Hancock. Approximate von neumann entropy for directed graphs. *Physical Review E*, 89(5):052804, 2014.

Yihang Yin, Qingzhong Wang, Siyu Huang, Haoyi Xiong, and Xiang Zhang. Autogcl: Automated graph contrastive learning via learnable view generators. In *Proceedings of the AAAI Conference on Artificial Intelligence*, volume 36, pp. 8892–8900, 2022.

Yuning You, Tianlong Chen, Yongduo Sui, Ting Chen, Zhangyang Wang, and Yang Shen. Graph contrastive learning with augmentations. *Advances in Neural Information Processing Systems*, 33:5812–5823, 2020.

Yuning You, Tianlong Chen, Yang Shen, and Zhangyang Wang. Graph contrastive learning automated. In *International Conference on Machine Learning*, pp. 12121–12132. PMLR, 2021.

Junchi Yu, Tingyang Xu, Yu Rong, Yatao Bian, Junzhou Huang, and Ran He. Recognizing predictive substructures with subgraph information bottleneck. *IEEE Transactions on Pattern Analysis and Machine Intelligence*, 2021.

Jiaqi Zeng and Pengtao Xie. Contrastive self-supervised learning for graph classification. In *Proceedings of the AAAI Conference on Artificial Intelligence*, volume 35, pp. 10824–10832, 2021.

Liang Zeng, Lanqing Li, Ziqi Gao, Peilin Zhao, and Jian Li. Imgcl: Revisiting graph contrastive learning on imbalanced node classification. In *Proceedings of the AAAI Conference on Artificial Intelligence*, volume 37, pp. 11138–11146, 2023.

Hengrui Zhang, Qitian Wu, Junchi Yan, David Wipf, and Philip S Yu. From canonical correlation analysis to self-supervised graph neural networks. *Advances in Neural Information Processing Systems*, 34:76–89, 2021a.

Yifei Zhang, Hao Zhu, Zixing Song, Piotr Koniusz, and Irwin King. Spectral feature augmentation for graph contrastive learning and beyond. In *Proceedings of the AAAI Conference on Artificial Intelligence*, volume 37, pp. 11289–11297, 2023.

Zaixi Zhang, Qi Liu, Hao Wang, Chengqiang Lu, and Chee-Kong Lee. Motif-based graph self-supervised learning for molecular property prediction. *Advances in Neural Information Processing Systems*, 34:15870–15882, 2021b.

Han Zhao, Xu Yang, Zhenru Wang, Erkun Yang, and Cheng Deng. Graph debiased contrastive learning with joint representation clustering. In *IJCAI*, pp. 3434–3440, 2021.

Dongcheng Zou, Hao Peng, Xiang Huang, Renyu Yang, Jianxin Li, Jia Wu, Chunyang Liu, and Philip S Yu. Se-gsl: A general and effective graph structure learning framework through structural entropy optimization. *arXiv preprint arXiv:2303.09778*, 2023.

A Appendix

A.1 Notations

The main notations used in this paper are shown in Table 5.

Table 5: Notations

Symbol	Description	Symbol	Description
G	a graph	V	vertex set of graph G
$\mathbf{g}$	graph-level representation of G	n	the number of vertices of G
$\boldsymbol{Z}$	node representations matrix of G	$\boldsymbol{z}_i$	representation of node i
(G, P)	a probabilistic graph	$P(\mathbf{g}, \boldsymbol{Z})$	probability distribution on V
VP(G)	vertex packing polytope of G	$P_i(\mathbf{g}, \boldsymbol{Z})$	probability density of vertex i
$H_k(G, P)$	graph entropy	$H(P)$	Shannon entropy
$H_c(G, P, \boldsymbol{\pi})$	the entropy of a coloring $\boldsymbol{\pi}$	$H_\chi(G, P)$	chromatic entropy
$\boldsymbol{\pi}$	a coloring on vertex set V	$\boldsymbol{\Pi}(G)$	set of all coloring $\boldsymbol{\pi}$ of G
$\mathbb{C}_k$	the set of vertices with color k	$\alpha(G)$	the independence number of G
$\chi(G)$	the chromatic number of G	$D(G, P)$	gap between bounds of $H_k(G, P)$
θ	the parameters for learning $\mathbf{g}$	ϕ	the parameters for learning $\boldsymbol{Z}$
ψ	the parameters for learning $\boldsymbol{\pi}$	δ	error bound of the approximation

A.2 Error bound analysis of the approximation

Corollary A.1. *Let $\epsilon = \frac{\log \chi(G)}{1+\delta} + \log \alpha(G)$, if $H(P) \geq \epsilon$, we have $\frac{|H_k(G,P) - \hat{H}_k(G,P)|}{H_k(G,P)} \leq \delta$.*

Proof. Let $D(G, P)$ be the gap between lower and upper bounds in Theorem 2.8, we have

$$D(G, P) := H_\chi(G, P) - H(P) + \log \alpha(G). \tag{24}$$

Let $\chi(G)$ be chromatic number of graph G which is the smallest number of colors needed to color the vertices. The gap $D(G, P)$ is bounded by $\chi(G)$, $\alpha(G)$ and Shannon entropy $H(P)$ as follows.

Corollary A.2 (Cardinal et al. (2004; 2005))**.**

$$0 \leq D(G, P) \leq \log \chi(G) + \log \alpha(G) - H(P).$$

Let $\hat{\mu}$ be an estimator of μ and $\hat{H}_k(G, P)$ be an approximation of $H_k(G, P)$ with respect to $\hat{\mu}$. Suppose $H(P) - \log \alpha(G) > 0$, the error bound of the approximation is as follows

$$\frac{|H_k(G, P) - \hat{H}_k(G, P)|}{H_k(G, P)} \leq \frac{D(G, P)}{H(P) - \log \alpha(G)} \leq \frac{\log \chi(G)}{H(P) - \log \alpha(G)} - 1. \tag{25}$$

Since $\alpha(G)$ and $\chi(G)$ are constants of a given G, maximizing the Shannon entropy $H(P)$ is to minimize the upper bound of the error bound in equation 25 such that it yields a more exact approximation. Let δ be the upper bound of the error bound of our approximation, we have

$$\frac{\log \chi(G)}{H(P) - \log \alpha(G)} - 1 \leq \delta \Rightarrow H(P) \geq \frac{\log \chi(G)}{1 + \delta} + \log \alpha(G) \tag{26}$$

Thus, let $\epsilon = \frac{\log \chi(G)}{1+\delta} + \log \alpha(G)$, if $H(P) \geq \epsilon$, we have $\frac{|H_k(G,P) - \hat{H}_k(G,P)|}{H_k(G,P)} \leq \delta$. □

A.3 Architecture and Generalization

In this section, we introduce the architecture of our GeMax method is in Figure 2. In Figure 3, we apply GeMax on the architecture of InfoGraph by replacing the InfoMax loss with our GeMax objective $J(\mathcal{G}; \boldsymbol{\theta}, \boldsymbol{\phi}, \boldsymbol{\psi})$. In Figure 4, we show the architecture of Infograph Sun et al. (2019).

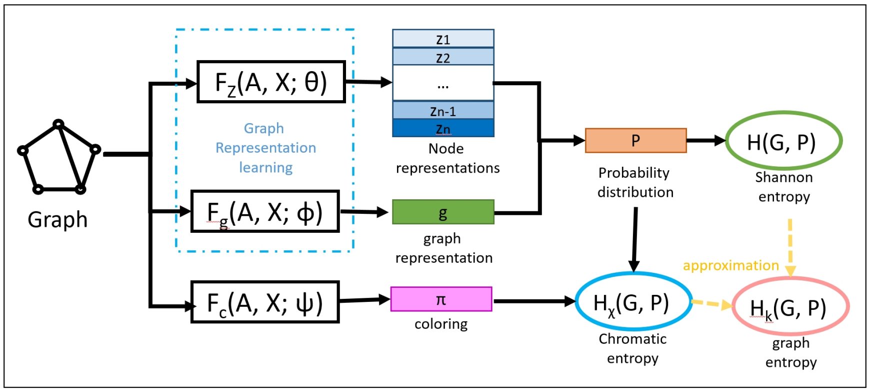

Figure 2: Architecture of GeMax

The graph representations learning part ($F_Z(\boldsymbol{A}, \boldsymbol{X}; \boldsymbol{\theta})$ and $F_g(\boldsymbol{A}, \boldsymbol{X}; \boldsymbol{\phi})$) in the blue dash box are not confined to any specific GNN models. Thus, GeMax can be applied on various GNN based models like InfoGraph Sun et al. (2019) or GraphCL You et al. (2020).

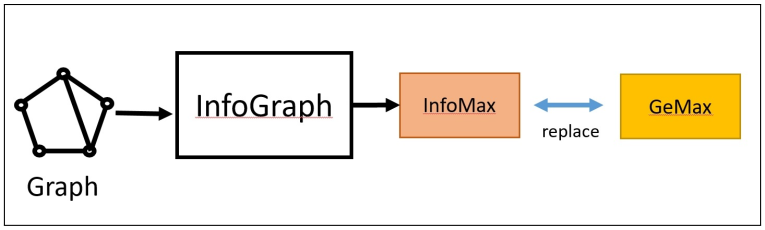

Figure 3: Applying GeMax to InfoGraph network by replacing the InfoMax loss

Given an unsupervised graph representation learning models, GeMax method is to replace the original loss with our GeMax objective $J(\mathcal{G}; \boldsymbol{\theta}, \boldsymbol{\phi}, \boldsymbol{\psi})$ equation 20 and introduce a coloring function $F_c(\boldsymbol{A}, \boldsymbol{X}; \boldsymbol{\psi})$. The $J(\mathcal{G}; \boldsymbol{\theta}, \boldsymbol{\phi}, \boldsymbol{\psi})$ can be optimized by our iterative algorithm.

A.4 EXPERIMENT: STATISTICS OF DATASET

In this section, we provide the statistics of the dataset we used in experiments. For graph-level representation learning tasks, we use the TUdataset Morris et al. (2020) in Table 6. For node-level representation learning tasks, we use the network dataset Sen et al. (2008) in Table 7 for edge prediction. The TUdataset used in graph-level

Table 6: Statistics of TUdataset Morris et al. (2020)

Name	Num. of graphs	Num. of classes	Num. of nodes	node labels	node attributes
MUTAG	188	2	17.9	yes	no
PROTEINS	1113	2	39.1	yes	yes
DD	1178	2	284.32	yes	no
NCI1	4110	2	29.9	yes	no
COLLAB	5000	3	74.49	no	no
IMDB-B	1000	2	19.8	no	no
REDDIT-B	2000	2	429.63	no	no
REDDIT-M5K	4999	5	508.52	no	no
GITHUB	12725	2	113.79	no	no

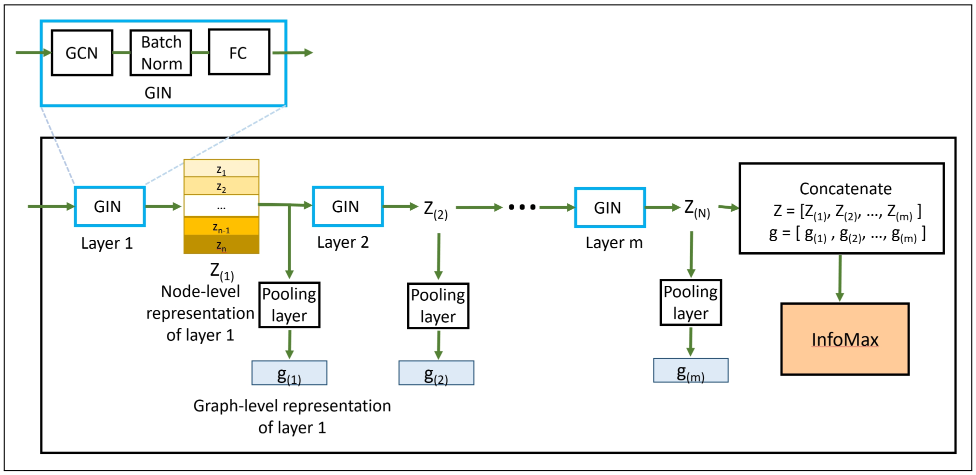

Figure 4: Architecture of InfoGraph with m layers

Table 7: Statistics of Network dataset Sen et al. (2008) for edge prediction

Name	Num. of nodes	Num. of node class	Num. of edges	described by a 0/1-valued
Cora	2708	7	5429	yes
Citeseer	3312	6	4732	yes
Pubmed	19717	3	44338	yes

A.5 EXPERIMENT BASELINE: INFORMAX METHODS

For unsupervised and semi-supervised graph-level learning, those InfoMax based methods are the most current and influential methods spanning from 2019 to 2022, each boasting high citations on Google Scholar (see Table 8). Besides the InfoMax principle, there are few works on graph information bottleneck (GIB) Wu et al. (2020) and the subgraph information bottleneck (SIB) Yu et al. (2021). GIB and SIB aim to learn the minimal sufficient representation for downstream tasks. But GIB Wu et al. (2020) and SIB Yu et al. (2021) may fail if the downstream tasks are not available in the representation learning stage. Thus they are not suitable for unsupervised and semi-supervised graph learning such that they are not included in our baselines. To the best of our knowledge, we don't find other principles for unsupervised graph-level representation learning except InfoMax, GIB and SIB. Since the InfoMax methods are the most influential methods, we compare with them by replacing the InfoMax objective with our GeMax objective in equation 20 (see Figure 2 and Figure 3). In this work, we compare with five InfoMax based methods, that is, InfoGraph (Sun et al., 2019), GraphCL (You et al., 2020), AD-GCL (Suresh et al., 2021), JOAO (You et al., 2021) , AutoGCL (Yin et al., 2022). All these five methods share the same graph representation learning architecture with InfoGraph Sun et al. (2019), as shown in Figure 4.

Table 8: Google scholar citations comparison

principle	InfoMax					GIB	SIB
methods	InfoGraph	GraphCL	AD-GCL	JOAO	AutoGCL		
citations	665	1101	176	249	42	129	26

Following (Nowozin et al., 2016; Sun et al., 2019; Belghazi et al., 2018), suppose the node-level representation $\boldsymbol{z}_p(x)$ and the graph-level representation $\boldsymbol{g}(x)$ are depending on the input x, T_φ is a discriminator parameterized by a neural network with parameters φ, the Jensen-Shannon mutual information (MI) estimator (Fuglede & Topsoe, 2004; Nowozin et al., 2016; Hjelm et al., 2019; Sun et al., 2019) I_φ between $\boldsymbol{z}_v$ and $\boldsymbol{g}$ is defined as

$$I_\varphi(\boldsymbol{z}_p, \boldsymbol{g}) = \mathbb{E}_{\mathbb{P}}[-\mathrm{sp}(-T_\varphi(\boldsymbol{z}_p(x), \boldsymbol{g}(x)))] - \mathbb{E}_{\mathbb{P}\times\tilde{\mathbb{P}}}[\mathrm{sp}(T_\varphi(\boldsymbol{z}_p(x'), \boldsymbol{g}(x)))], \tag{27}$$

where x is the input sample from distribution $\mathbb{P}$, x' is the negative sample from distribution $\tilde{\mathbb{P}}$, and $\mathrm{sp}(a) = \log(1 + e^a)$ denotes the softplus function. $\mathbb{P}$ is the empirical probability distribution of the input space and $\tilde{\mathbb{P}}$ is the empirical probability distribution of the negative input space. Many recent graph-level representation learning methods (Sun et al., 2019; You et al., 2020; Yin et al., 2022) are based on the InfoMax principle, i.e., maximizing equation 27. For example, InfoGraphSun et al. (2019) obtains graph-level representations by maximizing the mutual information between the graph-level representation and the node-level representations as follows

$$\phi^*, \theta^*, \varphi^* = \underset{\phi,\theta,\varphi}{\arg\max} \sum_{i=1}^{|\mathcal{G}|} \frac{1}{|V_i|} \sum_{p\in V_i} I_\varphi(\boldsymbol{z}_p^\theta, \boldsymbol{g}_i^\phi), \tag{28}$$

where I_φ is the Jensen-Shannon MI estimator defined by equation 27. For semi-supervised learning, the dataset $\mathcal{G}$ is split into labeled dataset $\mathcal{G}^L$ and unlabeled dataset $\mathcal{G}^U$. They deploy another supervised encoder with parameter ψ and then generate the supervised node-level representations $\boldsymbol{Z}_i^\psi$, graph-level representations $\boldsymbol{g}_i^\psi$ and prediction $\hat{\boldsymbol{y}}_i^\psi$. The loss function of InfoGraph for semi-supervised learning is defined as follows:

$$\mathcal{L}_{\text{info-semi}} = \sum_{l=1}^{|\mathcal{G}^L|} \mathcal{L}_{\text{supervised}}(\hat{\boldsymbol{y}}_l^\psi, \boldsymbol{y}_l) + \sum_{i=1}^{|\mathcal{G}|} \mathcal{L}_{\text{unsupervised}}(\boldsymbol{Z}_i^\theta, \boldsymbol{g}_i^\phi) - \lambda \sum_{i=1}^{|\mathcal{G}|} \frac{1}{|V_i|} I_\varphi(\boldsymbol{g}_i^\phi, \boldsymbol{g}_i^\psi) \tag{29}$$

where $\mathcal{L}_{\text{unsupervised}}$ is derived from equation 28. The last term encourages the representations learned by the two encoders to have high mutual information.

A.6 EXPERIMENT: GRAPH-LEVEL TASKS

Unsupervised learning Following (Sun et al., 2019; You et al., 2021; Yin et al., 2022), we train a graph representation model on unlabeled data to obtain graph representations and use these representations and graph labels to train a SVM classifier. Our experimental setup follows AutoGCL (Yin et al., 2022). Actually, all the four InfoMax methods (GraphCL, AD-GCL, JOJOv2 and AutoGCL) are based on the architecture of InfoGraph. Specifically, they use a 5-layer GIN Xu et al. (2018) with hidden size 128 as the representation model, shown in Figure 4. The model is trained with a batch size of 128 and a learning rate of 0.001. For those contrastive learning methods (e.g., JOJOv2 and AutoGCL), they use 30 epochs of contrastive pre-training under the naive strategy. We repeat the experiments for 10 times with different random seeds. In each time, we perform 10-fold cross-validation on each dataset. Specifically, in each fold, we use 90% of the total data as unlabeled data for contrastive pre-training and 10% as labeled testing data. The hyperparameters of Algorithm 1 are $\mu^0 = 0.5, \gamma = 0.5, \eta = 0.5, \epsilon = 0.3 \log n, \tau = 0.01$. We also conduct sensitivity analysis in Appendix A.8 to study how different hyperparameters affect the results. The average accuracy (ACC) and standard deviation are reported in Table 14.

Semi-supervised Learning Following (Hu et al., 2019; You et al., 2021; Yin et al., 2022), we compare our GeMax methods with InfoMax-based methods in semi-supervised learning tasks. The semi-supervised losses of InfoMax based methods were shown in equation 29 of Appendix A.5. To ensure fair comparisons, we follow the semi-supervised learning of InfoMax methods in equation 29 and replace the InfoMax objective with our GeMax objective in equation 20. Following the settings of AutoGCL (Yin et al., 2022), we employ a 10-fold cross-validation on each dataset. For each fold, we use 80% of the total data as the unlabeled data, 10% as labeled training data, and 10% as labeled testing data. The classifier for labeled data is a ResGCN (Chen et al., 2019) with 5 layers and a hidden size of 128. We repeat each experiment 10 times and report the average accuracy in Table 2.

A.7 EXPERIMENT: NODE-LEVEL TASKS

Though original motivation of orthonormal representations in equation 1 is from information theory, it can be used to reconstruct the adjacency matrix $\boldsymbol{A}$ using the information of non-adjacency.

Denoting $\hat{\boldsymbol{A}}$ as the reconstructed adjacency matrix, we have

$$\hat{\boldsymbol{A}} = \sigma(\mathbf{abs}(\boldsymbol{Z}^{\phi}(\boldsymbol{Z}^{\phi})^{\top} - \boldsymbol{I}_n)), \tag{30}$$

where the $\mathbf{abs}(\cdot)$ is the element-wise absolute value function and the $\sigma(\cdot)$ is a element-wise sigmoid function. Thus, we can compare our GeMax methods with other graph reconstruction methods such as VGAE Kipf & Welling (2016b), ARGA Pan et al. (2018), GIC Mavromatis & Karypis (2020) and LGAE Salha et al. (2021). We use the network architecture of InfoMax methods (InfoGraph, GraphCL and AutoGCL) by replacing the InfoMax objective with our GeMax objective. Since the orthonormal representations mainly contributes to graph reconstruction and edge prediction, we should set the parameter of orthonormal representations regularization (i.e., η) larger. The hyperparameters of Algorithm 1 are $\mu^0 = 0.5, \gamma = 0.5, \eta = 5, \epsilon = 0.3 \log n, \tau = 0.01$.

Following VGAE Kipf & Welling (2016b), all the models are trained on an incomplete version of these datasets where parts of the edges have been removed, while all node features are kept. We split the nodes of each dataset into three parts: 80% as training set, 10% as validation set and 10% as test set. We report area under the ROC curve (AUC) and average precision (AP) scores for each model on the test set in Table 4.

A.8 EXPERIMENT: SENSITIVITY ANALYSIS OF HYPERPARAMETERS

In the alternative algorithm 1, there are four hyperparameters need to be tuned: the initial approximation weight μ^0, the orthonormal representation regularization parameter γ, the coloring regularization parameter η, the lower threshold of average Shannon entropy ϵ. In this section we analyse the parameter sensitivity on the InfoGraph Sun et al. (2019) with different hyperparameters. We repeat each experiments for ten times and plot the average accuracy with variance on different datasets.

A.8.1 THE INITIAL APPROXIMATION WEIGHT

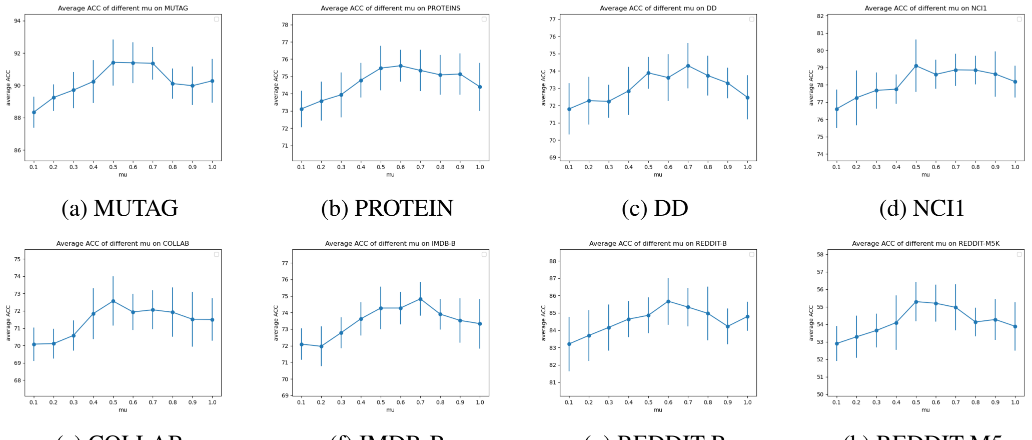

(a) MUTAG (b) PROTEIN (c) DD (d) NCI1

(e) COLLAB (f) IMDB-B (g) REDDIT-B (h) REDDIT-M5

Figure 5: The average ACC of different μ on different data

The approximation weight μ is initialized as $\mu = \mu^0$ in the beginning of algorithm 1. In Figure 5, we fix $\epsilon = 0.3 \log n$ and other hyperparameters. We tune μ^0 from $\{0.1, 0.2, ..., 0.9, 1\}$. The results show that algorithm 1 achieves the top performance when $0.5 \leq \mu^0 \leq 0.7$. If $\mu^0 = 0$, the approximation to the graph entropy starts with $\hat{H}_k(G, P) = H_c(G_j, P(\mathbf{g}_j^{\theta^0}, \boldsymbol{Z}_j^{\phi^0}), \boldsymbol{\pi}^{\psi^0})$. However, a very small μ^0 adversely affect the performance because the coloring $\boldsymbol{\pi}^{\psi^0}$ is randomly initialized in the beginning. If $\mu^0 = 1$, the algorithm 1 degenerates to equation 11, that is, maximizing the lower bound of graph entropy. If the equality in Corollary 2.9 holds, $\mu^0 = 1$ can result in learning the representations for exact graph entropy $H_k(G, P)$. However, if the equality in Corollary 2.9 doesn't hold, the approximation will be inexact and thus the performance decreases.

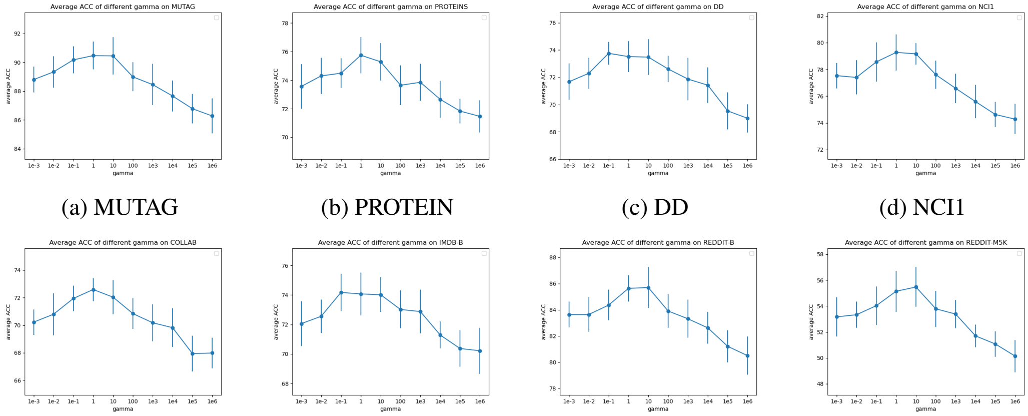

(a) MUTAG (b) PROTEIN (c) DD (d) NCI1

(e) COLLAB (f) IMDB-B (g) REDDIT-B (h) REDDIT-M5

Figure 6: The average ACC of different γ on different data

A.8.2 THE ORTHONORMAL REPRESENTATION REGULARIZATION PARAMETER

γ is the hyperparameter for orthonormal representation regularization. In Figure 6, we fix other hyperparameters and tune γ from $\{10^{-3}, 10^{-2}, ..., 10^5, 10^6\}$. The results show that γ is not sensitive when $1 \leq \gamma \leq 10$. If γ is too small, the performance decreases because the node-level representations $\boldsymbol{Z}$ may not be orthonormal representations. A very large γ adversely affect the performance because the orthonormal representation regularization dominates the representation learning.

A.8.3 THE COLORING REGULARIZATION PARAMETER

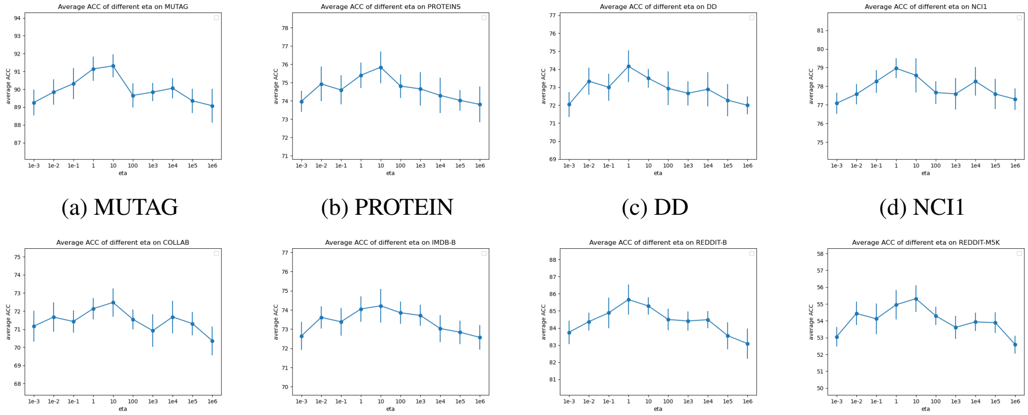

(a) MUTAG (b) PROTEIN (c) DD (d) NCI1

(e) COLLAB (f) IMDB-B (g) REDDIT-B (h) REDDIT-M5

Figure 7: The average ACC of different η on different data

η is the hyperparameter for coloring regularization. In Figure 7, we fix other hyperparameters and tune η from $\{10^{-3}, 10^{-2}, ..., 10^5, 10^6\}$. The results show that algorithm 1 achieve top comference when $1 \leq \eta \leq 10$. If η is too small, the performance decreases because the the coloring function F_c are unable to search for a coloring for G. A very large η adversely affect the performance because the coloring searched by F_c is not related to the chromatic entropy.

A.8.4 THE LOWER THRESHOLD OF AVERAGE SHANNON ENTROPY

In algorithm 1, we use ϵ to control the updating of μ. In Figure 8, we fix other hyperparameters and tune ϵ ranging from $0.1 \log n$ to $\log n$. The results show that ϵ is not sensitive when $0.3 \leq \epsilon \leq 0.4$.

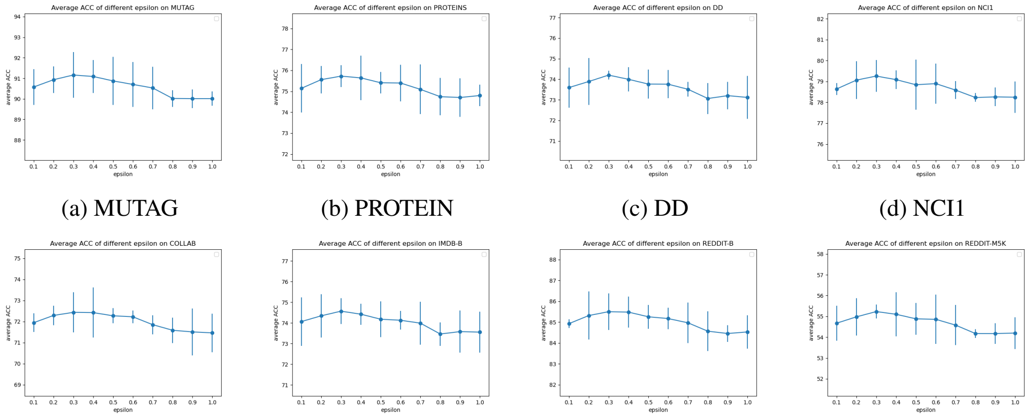

(a) MUTAG (b) PROTEIN (c) DD (d) NCI1

(e) COLLAB (f) IMDB-B (g) REDDIT-B (h) REDDIT-M5

Figure 8: The average ACC of different ϵ on different data

If ϵ is too small, the algorithm 1 degenerates to equation 11, that is, maximizing the lower bound of graph entropy. If the equality in Corollary 2.9 holds, $\mu^0 = 1$ can result in learning the representations for exact graph entropy $H_k(G, P)$. However, if the equality in Corollary 2.9 doesn't hold, the approximation will be inexact and thus the performance decreases. If ϵ is large, the μ will not be updated such that the error bound are not guaranteed to be smaller than δ. Thus the performance decreases.

A.9 EXPERIMENT: ABLATION STUDY

In the ablation study, we analyse the importance of each part of GeMax objective $J(\mathcal{G}; \boldsymbol{\theta}, \boldsymbol{\phi}, \boldsymbol{\psi})$.

A.9.1 REMOVE THE ORTHONORMAL REPRESENTATION REGULARIZATION

We remove the orthonormal representation regularization of GeMax objective $J(\mathcal{G}; \boldsymbol{\theta}, \boldsymbol{\phi}, \boldsymbol{\psi})$ in equation 20 by setting $\gamma = 0$. The results in Table 9 show that the orthonormal representation regularization can improve the performance of graph representation learning.

Table 9: Performance (ACC) of unsupervised learning for Ablation study. The ablation indicates $\gamma = 0$ in equation 20. The **bold** numbers denote the better performances of the same method.

methods	ablation	MUTAG	PROTEINS	DD	NCI1	COLLAB	IMDB-B	REDDIT-B	REDDIT-M5K
InfoGraph	✓	87.48±1.56	73.29±1.13	72.54±1.27	76.89±1.28	70.22±1.97	71.53±1.31	84.07±1.16	54.32±1.53
	×	**91.13±1.70**	**75.77±1.26**	**74.16±1.65**	**79.24±1.43**	**72.57±1.74**	**74.59±1.53**	**85.53±1.92**	**55.21±1.69**
GraphCL	✓	88.39±1.12	74.43±1.28	76.77±1.22	76.09±1.26	70.32±1.85	71.07±1.36	88.73±1.52	54.69±1.49
	×	**90.36±1.69**	**76.86±1.62**	**79.25±1.53**	**78.72±1.79**	**73.43±1.62**	**73.12±1.25**	**91.47±1.74**	**56.25±1.53**
AD-GCL	✓	87.45±1.31	73.01±1.55	76.23±1.86	74.73±1.19	72.85±1.37	71.64±1.13	86.65±1.28	54.91±1.59
	×	**89.68±1.47**	**74.52±1.71**	**77.58±1.41**	**76.35±1.62**	**74.83±1.79**	**73.52±1.45**	**88.03±1.62**	**55.03±1.54**
JOAOv2	✓	87.69±1.81	73.05±1.16	70.03±1.83	72.67±1.98	70.11±1.50	71.37±1.56	80.24±1.35	55.42±1.33
	×	**88.33±1.58**	**74.63±1.87**	**72.60±1.35**	**75.36±1.42**	**71.68±1.67**	**72.21±1.72**	**81.68±1.40**	**57.17±1.67**
AutoGCL	✓	87.23±1.48	74.36±1.65	76.79±1.60	81.76±1.55	70.48±1.08	72.63±1.54	87.03±1.95	54.27±1.61
	×	**90.85±1.28**	**76.23±1.29**	**78.36±1.51**	**83.21±1.34**	**72.39±1.57**	**74.05±1.79**	**90.42±1.31**	**56.81±1.85**

A.9.2 REMOVE THE GRAPH ENTROPY

We remove the graph entropy of GeMax objective $J(\mathcal{G}; \boldsymbol{\theta}, \boldsymbol{\phi}, \boldsymbol{\psi})$ in equation 20 by setting $\gamma = 10^5$ such that the orthonormal representation will dominate the optimization. The results in Table 10 show that the graph entropy can improve the performance of graph representation learning.

A.9.3 REMOVE THE CHROMATIC ENTROPY

We remove the chromatic entropy of GeMax objective $J(\mathcal{G}; \boldsymbol{\theta}, \boldsymbol{\phi}, \boldsymbol{\psi})$ in equation 20 by setting $\mu = 1$. The results in Table 11 show that the chromatic entropy can improve the performance of graph representation learning.

Table 10: Performance (ACC) of unsupervised learning for Ablation study. The ablation indicates $\gamma = 10^5$ in equation 20. The **bold** numbers denote the better performances of the same method.

methods	ablation	MUTAG	PROTEINS	DD	NCI1	COLLAB	IMDB-B	REDDIT-B	REDDIT-M5K
InfoGraph	✓	82.53±1.24	70.57±1.42	71.18±1.34	73.26±1.45	68.73±1.43	70.11±1.09	82.43±1.24	51.53±1.42
	×	**91.13±1.70**	**75.77±1.26**	**74.16±1.65**	**79.24±1.43**	**72.57±1.74**	**74.59±1.53**	**85.53±1.92**	**55.21±1.69**
GraphCL	✓	83.54±1.47	71.39±1.65	73.26±1.03	75.86±1.31	69.07±1.37	70.22±1.87	85.98±1.47	52.37±1.50
	×	**90.36±1.69**	**76.86±1.62**	**79.25±1.53**	**78.72±1.79**	**73.43±1.62**	**73.12±1.25**	**91.47±1.74**	**56.25±1.53**
AD-GCL	✓	85.49±1.84	70.16±1.36	74.49±1.78	71.05±1.32	70.58±1.73	70.90±1.65	83.47±1.67	52.64±1.83
	×	**89.68±1.47**	**74.52±1.71**	**77.58±1.41**	**76.35±1.62**	**74.83±1.79**	**73.52±1.45**	**88.03±1.62**	**55.03±1.54**
JOAOv2	✓	82.73±1.69	70.48±1.43	68.24±1.69	70.04±1.25	69.27±1.47	70.63±1.04	78.15±1.57	52.79±1.27
	×	**88.33±1.58**	**74.63±1.87**	**72.60±1.35**	**75.36±1.42**	**71.68±1.67**	**72.21±1.72**	**81.68±1.40**	**57.17±1.67**
AutoGCL	✓	83.14±1.58	71.93±1.82	74.35±1.51	79.11±1.57	68.26±1.83	71.48±1.57	82.83±1.72	53.07±1.63
	×	**90.85±1.28**	**76.23±1.29**	**78.36±1.51**	**83.21±1.34**	**72.39±1.57**	**74.05±1.79**	**90.42±1.31**	**56.81±1.85**

Table 11: Performance (ACC) of unsupervised learning for Ablation study. The ablation indicates $\mu = 1$ in equation 20. The **bold** numbers denote the better performances of the same method.

methods	ablation	MUTAG	PROTEINS	DD	NCI1	COLLAB	IMDB-B	REDDIT-B	REDDIT-M5K
InfoGraph	✓	88.52±1.49	74.16±1.37	72.98±1.52	78.30±1.67	71.95±1.43	72.46±1.08	84.91±1.34	54.96±1.53
	×	**91.13±1.70**	**75.77±1.26**	**74.16±1.65**	**79.24±1.43**	**72.57±1.74**	**74.59±1.53**	**85.53±1.92**	**55.21±1.69**
GraphCL	✓	89.27±1.54	75.16±1.43	77.73±1.28	77.19±1.69	72.21±1.54	72.21±1.21	90.34±1.86	55.10±1.88
	×	**90.36±1.69**	**76.86±1.62**	**79.25±1.53**	**78.72±1.79**	**73.43±1.62**	**73.12±1.25**	**91.47±1.74**	**56.25±1.53**
AD-GCL	✓	88.98±1.06	73.89±1.38	76.95±1.53	75.27±1.93	73.04±1.53	72.45±1.22	87.11±1.90	54.71±1.34
	×	**89.68±1.47**	**74.52±1.71**	**77.58±1.41**	**76.35±1.62**	**74.83±1.79**	**73.52±1.45**	**88.03±1.62**	**55.03±1.54**
JOAOv2	✓	87.52±1.69	73.79±1.93	71.52±1.58	74.70±1.31	71.19±1.74	72.08±1.38	80.49±1.05	56.23±1.78
	×	**88.33±1.58**	**74.63±1.87**	**72.60±1.35**	**75.36±1.42**	**71.68±1.67**	**72.21±1.72**	**81.68±1.40**	**57.17±1.67**
AutoGCL	✓	88.43±1.62	75.03±1.71	76.72±1.89	82.89±1.47	71.97±1.72	73.21±1.43	89.14±1.76	54.86±1.49
	×	**90.85±1.28**	**76.23±1.29**	**78.36±1.51**	**83.21±1.34**	**72.39±1.57**	**74.05±1.79**	**90.42±1.31**	**56.81±1.85**

A.9.4 REMOVE THE SHANNON ENTROPY

We remove the Shannon entropy of GeMax objective $J(\mathcal{G}; \boldsymbol{\theta}, \boldsymbol{\phi}, \boldsymbol{\psi})$ in equation 20 by setting $\mu = 0$. The results in Table 12 show that the Shannon entropy can improve the performance of graph representation learning.

Table 12: Performance (ACC) of unsupervised learning for Ablation study. The ablation indicates $\mu = 0$ in equation 20. The **bold** numbers denote the better performances of the same method.

methods	ablation	MUTAG	PROTEINS	DD	NCI1	COLLAB	IMDB-B	REDDIT-B	REDDIT-M5K
InfoGraph	✓	87.26±1.79	74.64±1.71	71.18±1.43	75.96±1.57	71.45±1.53	72.01±1.86	84.25±1.87	54.68±1.93
	×	**91.13±1.70**	**75.77±1.26**	**74.16±1.65**	**79.24±1.43**	**72.57±1.74**	**74.59±1.53**	**85.53±1.92**	**55.21±1.69**
GraphCL	✓	88.90±1.30	73.93±1.75	77.65±1.34	76.28±1.49	71.82±1.44	71.69±1.20	87.16±1.35	53.78±1.51
	×	**90.36±1.69**	**76.86±1.62**	**79.25±1.53**	**78.72±1.79**	**73.43±1.62**	**73.12±1.25**	**91.47±1.74**	**56.25±1.53**
AD-GCL	✓	87.08±1.12	72.95±1.32	75.26±1.43	74.59±1.47	71.61±1.42	70.45±1.48	85.62±1.76	54.87±1.35
	×	**89.68±1.47**	**74.52±1.71**	**77.58±1.41**	**76.35±1.62**	**74.83±1.79**	**73.52±1.45**	**88.03±1.62**	**55.03±1.54**
JOAOv2	✓	86.47±1.57	72.74±1.32	71.38±1.19	73.53±1.47	68.21±1.83	70.21±1.84	78.35±1.47	53.08±1.43
	×	**88.33±1.58**	**74.63±1.87**	**72.60±1.35**	**75.36±1.42**	**71.68±1.67**	**72.21±1.72**	**81.68±1.40**	**57.17±1.67**
AutoGCL	✓	87.57±1.76	73.26±1.48	74.49±1.81	80.22±1.59	70.46±1.93	72.35±1.17	86.49±1.67	53.57±1.90
	×	**90.85±1.28**	**76.23±1.29**	**78.36±1.51**	**83.21±1.34**	**72.39±1.57**	**74.05±1.79**	**90.42±1.31**	**56.81±1.85**

A.10 EXPERIMENT: CONVERGENCE ANALYSIS

In Figure 9, we can see that the orthonormal representation loss ℓ_{orth} and the coloring loss ℓ_c decrease into a small value. The Shannon entropy $H(P)$ and the chromatic entropy $H_\chi(G, P)$ converge into a stable value. Thus, the overall objective $J(\mathcal{G}; \boldsymbol{\theta}, \boldsymbol{\phi}, \boldsymbol{\psi})$ converges.

A.11 EXPERIMENT: EXACT PENALTY METHOD

We propose a exact penalty algorithm 2 to solve the problem 14 as follows. As γ and η increasing into a large value, the constraints will be satisfied. We repeat the unsupervised experiments using algorithm 2 and report the results in Table 13. we have found that the representations given the regularized optimization are as good as those given by the constrained optimization.

A.12 EXPERIMENT: TIME COST

We run the programming on a machine with Intel 7 CPU and RTX 3090 GPU. We repeat the experiment for five times and report the results in Table **??**.

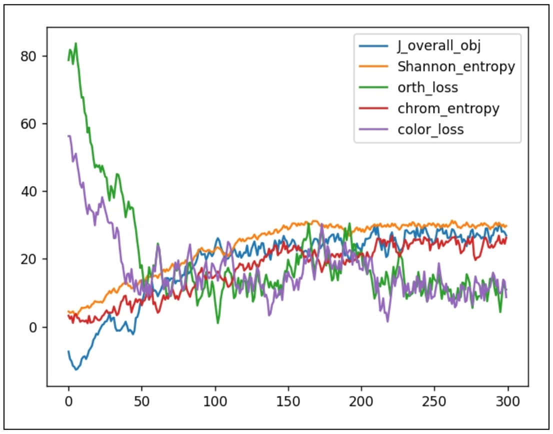

Figure 9: Convergence analysis of each part of the GeMax objective

Algorithm 2 exact penalty method

```
**Initialization:** $\boldsymbol{\theta}^0, \boldsymbol{\phi}^0, \boldsymbol{\psi}^0, \mu^0 = 0.5, \gamma = 0.5, \eta = 0.5, \epsilon$ (e.g., $0.3 \log n$), $\varepsilon$ (e.g., $0.01$).
**repeat**
    $\theta^{t+1}, \phi^{t+1} = \text{argmax}_{\theta,\phi}\, J(\mathcal{G}; \boldsymbol{\theta}, \boldsymbol{\phi}, \boldsymbol{\psi}^t)$
    $\boldsymbol{\psi}^{t+1} = \text{argmin}_{\boldsymbol{\psi}}\, J(\mathcal{G}; \boldsymbol{\theta}^{t+1}, \boldsymbol{\phi}^{t+1}, \boldsymbol{\psi})$
    $\gamma^{t+1} = \gamma^t + 0.005$, $\eta^{t+1} = \eta^t + 0.005$
    **if** $\bar{H}(\mathcal{G}; t) < \epsilon$ and $\mu^t + 0.01 \leq 1$ **then** $\mu^{t+1} = \mu^t + 0.01$ **else** $\mu^{t+1} = \mu^t$
**until** $|J(\mathcal{G}; \boldsymbol{\theta}^{t+1}, \boldsymbol{\phi}^{t+1}, \boldsymbol{\psi}^{t+1}) - J(\mathcal{G}; \boldsymbol{\theta}^t, \boldsymbol{\phi}^t, \boldsymbol{\psi}^t)| \leq \varepsilon$
```

Table 13: Performance (ACC) of unsupervised learning. regularized opt. denotes the regularized algorithm 1 and constrained opt. denotes the exact algorithm 2.The **bold** numbers denote the better performances of the same method.

methods	algorithm	MUTAG	PROTEINS	DD	NCI1
InfoGraph	regularized opt.	91.13±1.70	**75.77±1.26**	74.16±1.65	**79.24±1.43**
	constrained opt.	**91.67±1.52**	75.39±1.75	**75.21±1.70**	79.16±1.23
GraphCL	regularized opt.	**90.36±1.69**	**76.86±1.62**	79.25±1.53	78.72±1.79
	constrained opt.	90.05±1.87	76.04±1.91	**79.63±1.67**	**78.95±1.83**
AD-GCL	regularized opt.	**89.68±1.47**	74.52±1.71	77.58±1.41	**76.35±1.62**
	constrained opt.	89.25±1.52	**74.71±1.53**	**77.87±1.22**	75.73±1.29

Table 14: Time cost. The h is for hour and the m is for minute.

tasks	methods and principles		MUTAG	PROTEINS	DD	NCI1	COLLAB	IMDB-B	REDDIT-B	REDDIT-M5K
unsupervised learning	InfoGraph	InfoMax	2.2 m	11.3 m	1 h 32 m	38.1 m	1 h 36 m	4.7 m	3 h 16 m	7 h 25 m
		GeMax	2.4 m	12.7 m	1 h 26 m	37.2 m	1 h 48 m	5.2 m	3 h 27 m	7 h 47 m
	GraphCL	InfoMax	3.2 m	17.2 m	1 h 54 m	51.8 m	2 h 23 m	6.1 m	4 h 49 m	10 h 25 m
		GeMax	3.5 m	16.8 m	2 h 03 m	58.3 m	2 h 32 m	7.5 m	4 h 31 m	10 h 46 m
	AD-GCL	InfoMax	4.7 m	26.4 m	2 h 35 m	1h 7 m	2 h 48 m	15.5 m	5 h 37 m	14 h 16 m
		GeMax	4.5 m	25.1 m	2 h 42 m	1h 16 m	2 h 57 m	13.2 m	5 h 26 m	13 h 52 m
	JOAOv2	InfoMax	5.7 m	33.8 m	3 h 2 m	1h 29 m	3 h 10 m	23.6 m	6 h 7 m	15 h 35 m
		GeMax	6.4 m	35.2 m	3 h 18 m	1h 15 m	3 h 23 m	24.1 m	6 h 15 m	15 h 26 m
	AutoGCL	InfoMax	6.8 m	42.7 m	3 h 27 m	1h 56 m	3 h 47 m	32.4 m	6 h 35 m	16 h 43 m
		GeMax	6.3 m	41.2 m	3 h 34 m	2h 7 m	3 h 52 m	34.1 m	6 h 46 m	16 h 56 m
semi-supervised learning	InfoGraph	InfoMax	-	12.7 m	2 h 8 m	55.3 m	2 h 38 m	-	4 h 2 m	9 h 17 m
		GeMax	-	13.9 m	2 h 12 m	57.2 m	2 h 49 m	-	4 h 13 m	9 h 26 m
	GraphCL	InfoMax	-	23.4 m	2 h 45 m	1 h 7 m	2 h 42 m	-	5 h 36 m	12 h 7 m
		GeMax	-	25.3 m	2 h 57 m	1 h 13 m	2 h 56 m	-	5 h 43 m	12 h 23 m
	AD-GCL	InfoMax	-	35.1 m	3 h 24 m	1 h 39 m	3 h 15 m	-	6 h 26 m	14 h 33 m
		GeMax	-	38.6 m	3 h 17 m	1 h 49 m	3 h 21 m	-	6 h 43 m	14 h 47 m
	JOAOv2	InfoMax	-	43.8 m	3 h 31 m	2 h 1 m	4 h 23 m	-	7 h 12 m	17 h 26 m
		GeMax	-	46.2 m	3 h 49 m	2 h 17 m	4 h 18 m	-	7 h 29 m	17 h 49 m
	AutoGCL	InfoMax	-	49.3 m	3 h 40 m	2 h 13 m	4 h 28 m	-	7 h 36 m	18 h 56 m
		GeMax	-	53.4 m	3 h 54 m	2 h 27 m	4 h 39 m	-	7 h 41 m	18 h 15 m